



## Ceramics from Samshvilde (Georgia): A pilot archaeometric study

L. Randazzo <sup>a,1</sup>, E. Gliozzo <sup>a,1</sup>, M. Ricca <sup>a</sup>, N. Rovella <sup>a,\*</sup>, D. Berikashvili <sup>b</sup>, M.F. La Russa <sup>a,c</sup>

<sup>a</sup> Department of Biology, Ecology and Earth Sciences (DiBEST), University of Calabria, 87036 Arcavacata di Rende, Cosenza, Italy

<sup>b</sup> Department of Archaeology, Anthropology and Art of the University of Georgia, Kostavast. 77a, 0171 Tbilisi, Georgia

<sup>c</sup> Institute of Atmospheric Sciences and Climate, National Research Council, Via Gobetti 101, 40129 Bologna, Italy

### ARTICLE INFO

#### Keywords:

Prehistoric pottery  
Medieval pottery  
Lead glaze  
Tin glaze  
Alkali glaze  
Samshvilde  
Georgia

### ABSTRACT

This archaeometric study deals with seven samples of prehistoric pottery and, for the first time in Georgian studies, thirteen samples of glazed medieval pottery. All specimens were collected at Samshvilde, the most remarkable archaeological complex in southern Georgia and believed to represent locally-manufactured products. Two additional samples of raw materials composed of clay, silt, and sand were collected near the site and used to compare composition. Several analytical techniques were applied: Optical Microscopy (OM), Scanning Electron Microscopy (SEM), Electron Probe Microanalysis (EPMA), X-ray Diffraction (XRD) and X-ray Fluorescence (XRF). The results allowed to build a complex scenario in terms of exploitation of raw materials and technological choices. The raw materials indicate a volcanic environment and correspond to the geological settings of the territory of Samshvilde. The glazed ceramics were characterised as alkali, low alkali – low lead, lead, high lead and tin-opacified mixed-alkaline lead glazes. The compositional comparisons extend from east to west and place these ceramics in the wider framework of Islamic ceramics.

### 1. Introduction

Surrounded by other Caucasian regions (Turkey, Armenia, Azerbaijan and Russia), Georgia holds a key position for understanding the commercial dynamics within and among these territories and in relation to Near East civilizations.

The few archaeometric studies available mainly concern the lithic industry and metallurgy. Obsidian tools were the object of recent archaeological (Badalyan and Chataigner, 2004; Berikashvili and Coupal, 2018; Grigolia and Berikashvili, 2018; Sagona, 2018) and archaeometric research (Le Bourdonnec et al., 2012; Chataigner and Gratuze, 2014a; 2014b; Biagi and Gratuze, 2016; Biagi et al., 2017; La Russa et al., 2019). Conversely, the archaeometric literature on metallic objects is less consistent and mostly older (Kavtaradze, 1999; Schilling, 1997; Hauptmann and Klein, 2009; Stöllner and Gambashidze, 2014; Erb-Satullo, 2018).

As far as Georgian ceramics are concerned, only prehistoric finds have been investigated to date. Trojsi et al. (2002) and Kibaroglu et al. (2009) conducted mineralogical and petrographic analyses on a collection of sixteen Early Bronze Age ceramic samples from the settlements of Koda, Kiketi, Medamgreis Gora, Satkhe and Kvatskhelebi

(Fig. 1 nos. 1–5). Kibaroglu et al. (2009) performed petrographic and geochemical analysis on twenty Middle Bronze, Late Bronze/Early Iron Age ceramic samples from the archaeological sites of Udabno I (Fig. 1 no. 6) and Didi Gora (Fig. 1 no. 7) and on thirty-one clay samples in both the Sagaredjo district (Tetrobiani, Petrepauli, Patardzeuli and Karchana; Fig. 1 nos. 8–11) and the Alazani basin (Ichalto, Vardiskubani, Pona and Bodbizchevi; Fig. 1 nos. 12–15). In both cases, the sample sets were determined to be of local origin.

Excluding research by Shaar et al. (2017) on the “Levantine Iron Age geomagnetic anomaly” in Georgian pottery, the papers quoted above are the only two archaeometric studies on Georgian ceramics.

Given the small progress made in the field of Georgian ceramics, the present research was mostly exploratory. To design relevant research on Georgian ceramics, basic typological knowledge of local ceramic products is required; therefore, the archaeological site of Samshvilde was selected because of its potential as evidenced by the diachronic and heterogeneous character of its ceramic collection. The archaeometric study was aimed at characterising the main types of prehistoric and Medieval ceramics. This selection may be controversial; however, it is appropriate and functional because it focuses on the only two types of ceramics recognized as locally-made products. This research is,

\* Corresponding author.

E-mail address: [natalia.rovella@unical.it](mailto:natalia.rovella@unical.it) (N. Rovella).

<sup>1</sup> These Authors contributed equally to this study.

therefore, important to enable us to recognise imported ceramics and provide a guide for future study. The study applied several different techniques (OM, SEM, EPMA, XRD and XRF), as currently required (Amadori et al., 2017; Eramo, 2020; Gliozzo, 2020a; Hein and Kilikoglou, 2020; Ionescu and Hoeck, 2020; Montana, 2020; Pradell and Molera, 2020). This analytical protocol is suitable for obtaining both in situ and bulk data on tiny samples such as those available for this research.

## 2. Archaeological background

Samshvilde is one of the most remarkable archaeological complexes in southern Georgia and in Caucasia overall territory. Samshvilde is located on a promontory in the province of Kvemo Kartli (41°30'26"N, 44°30'20"E), close to the southern branch of the Silk Road (Berikashvili and Coupal, 2018). Its favourable geographical position was the main pull factor that attracted people to its centre since the Stone Age.

Seminal archaeological research projects were conducted during the Soviet period (Chilashvili, 1970) while systematic investigations began in 2012, through the work of the University of Georgia. The current research program is interdisciplinary and aimed to improve our understanding of site development through the ages. During seven field seasons, Neolithic, Bronze Age and Medieval phases of development were identified and materials recovered to date are the object of a combined archaeological and archaeometric study.

A brief overview of the main historical phases is provided to contextualise on-going archaeometric research on Georgian ceramics.

To begin with, the Middle-Late Bronze and Early Iron ages are supported by a high quantity of pottery found inside the citadel. In particular, a Late Bronze-Early Iron Age (13th-12th century BCE) burial site (trench no. 68, nearly 5 m below the ground level; Berikashvili and Coupal, 2019) contained a cist and several fragments of black polished pottery, decorated with various geometric motifs. The most interesting find was a large fragment of a jug with zoomorphic handle, representing

a wild goat (*Capra aegagrus*) or a Caucasian tur (*Capra caucasica*) with prominent horns.

The well-preserved condition of the medieval contents allowed the research to be explored systematically. The political and economic role of Samshvilde became increasingly important in the 5th century CE and coincided with the increasing power of the Sasanian Empire in the South Caucasus. The dominance of the Sasanians lasted until the 7th century and then succumbed to Arab rule. Since the mid 8th century (i.e. the foundation of the "Saamiro" of Tbilisi), the Arab Emir governed a large part of the Kvemo Kartli region; however, the impact of the Arab culture should have been minimal if we consider epigraphic documents such as the inscription on the east façade of the cathedral where the Byzantine Emperors Constantine V and Leo IV are referenced.

Beginning in the middle of 9<sup>th</sup> century CE, the Shiraki Bagratuni royal dynasty of Armenia reigned in Georgia. In the 10th century CE, Samshvilde was known as the capital of the Tashir-Dzoraget Kingdom until the conquest of the Lore fortress by David IV and the consequent fall of the kingdom in 1118.

The town of Samshvilde reached its peak in the 12th century CE, but the 'golden age' ended abruptly with the arrival of the Mongols in the 1230 s. Samshvilde was one of their main targets and suffered a progressive decline, culminating with the Tamerlane raids (1400–1403 CE) and the occupation by the Turkmen Shah Jahan (1440).

After dismemberment of the Kingdom of Kartli in the 16th-17th centuries AD (Kimiashvili, 1964), the town experienced a renaissance in the mid-18<sup>th</sup> century, slightly before its definitive abandonment.

Based on its history, it is clear that (a) Samshvilde is a complex and multicultural archaeological site with a diachronic but unbroken continuity from the Neolithic to the 18th century CE and (b) its study is of paramount importance as a source for the historical reconstruction of the entire Kvemo-Kartli region. The ceramic collection investigated here comes from the Samshvilde citadel (Fig. 2A, C) and the Sioni area (Fig. 2B).

The citadel was the main fortification system of Samshvilde. Built of basalt boulders and mortar, it consists of several building blocks

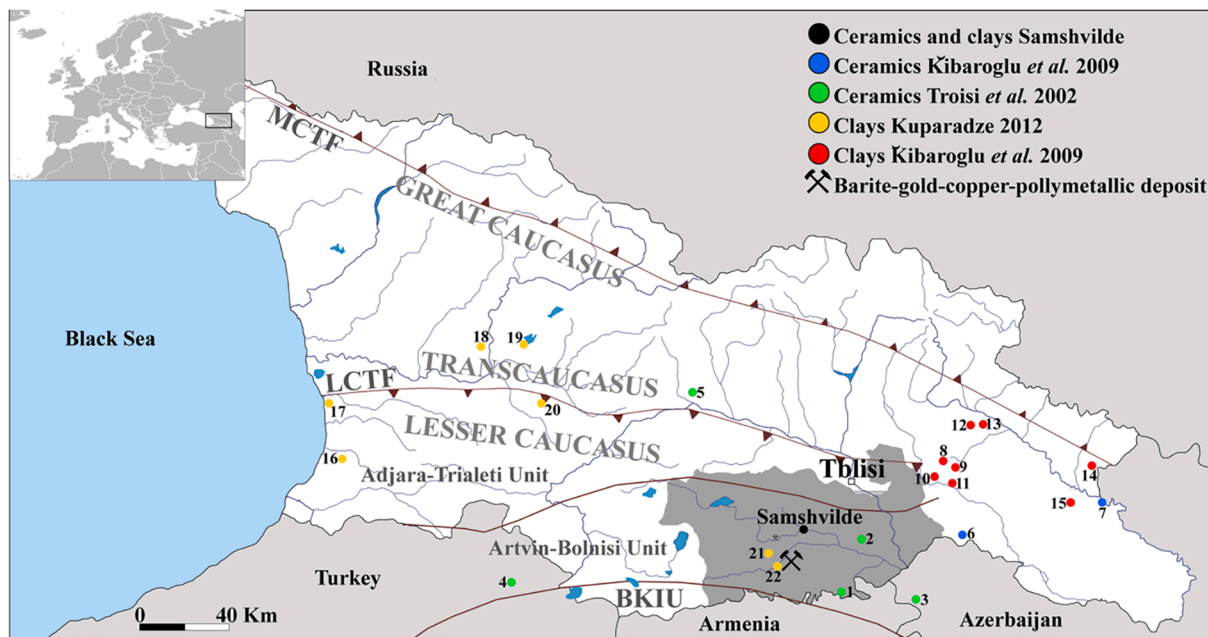


Fig. 1. The geographical location of Samshvilde in Georgia. The divisions among the Adjara-Trialeti, Baiburt-Karabakh and Artvin-Bolnisi Units have been drawn after Yilmaz et al. (2000). The MCTF (Main Caucasus Thrust Fault) and the LCTF (Lesser Caucasus Thrust Fault) have been drawn after Sokhadze et al. (2018). Dark grey areas indicate the present Kvemo-Kartli administrative region. Sites that have been the object of previous researches: 1-Koda, 2-Kiket, 3-Medamgreis Gora, 4-Satkhe and 5- Kvatskhelebi from Troisi et al. (2002); 6-Udabno I, 7-Didi Gora, 8-Tetrobiani, 9-Petrepauli, 10-Patardzeuli, 11-Karchana, 12-Ichalto, 13-Vardiskubani, 14-Pona and 15-Bodbizchevi from Kibaroglu et al. (2009); 16-Tsetskhlauri, 17-Makvaneti, 18-Rioni, 19-Tkibuli, 20-Shrosha, 21-Darbazi and 22-Dambludi-Mashavera from Kuparadze et al. (2012). Clay samples nearby the site no. 19 have been further investigated by Bertolotti and Kuparadze (2018).

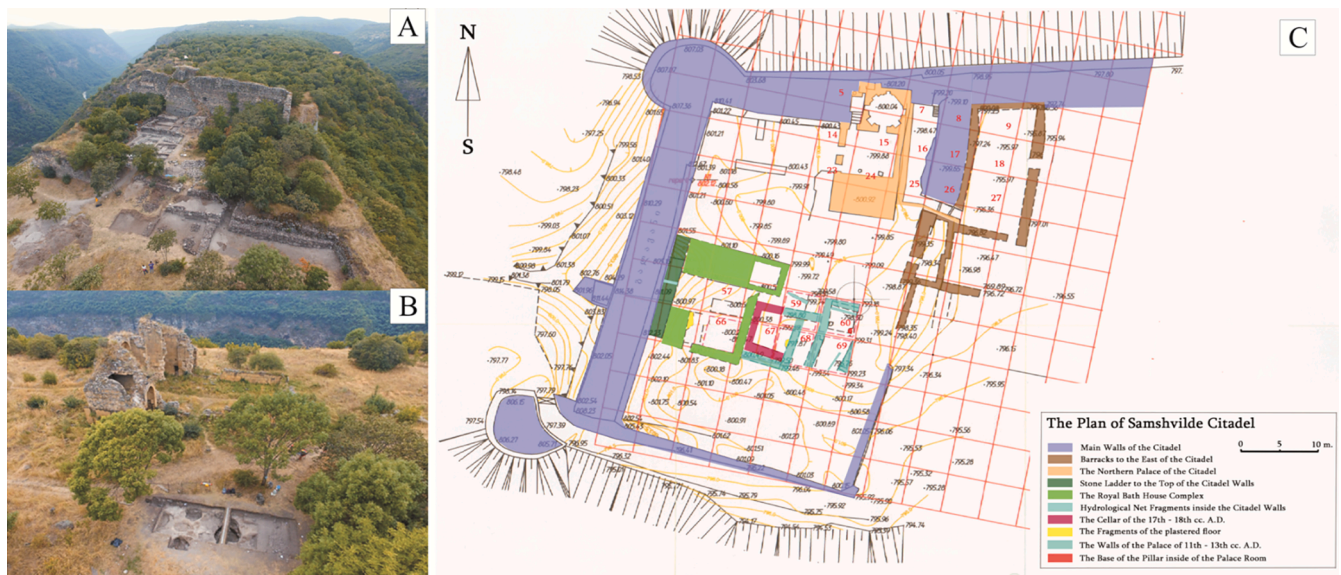


Fig. 2. Samshvilde citadel from the East (A); the Sioni Cathedral and the excavated area (B); Plan of Samshvilde citadel (C).

(frequently restructured and repaired) arranged in a rectangular shape. Inside the walls, the remains of a large structure (the ‘palace’) are located in the northern part and a similar but larger structure (possibly a warehouse) was found in the southern part. Between these two buildings, the baths were built, presumably in the 16th-17<sup>th</sup> centuries AD (Berikashvili and Pataridze, 2019).

Apart from the burial cist mentioned above, the archaeological excavation of the citadel has exhumed numerous stone, ceramic, glass and metal objects dated between the 5th and 18th centuries AD (Berikashvili and Pataridze, 2019).

The area of Sioni occupies the eastern sector of Samshvilde and corresponds to the surroundings of the 8th century CE homonymous cathedral. The architectural style is that of the so-called transitional period and the archaeological excavations recovered obsidian and argillite tools in lower Neolithic layers and a range of Bronze and Medieval pottery in the upper layers (Berikashvili et al., 2019).

### 3. Geological settings of the Kvemo-Kartli region

The archaeological site of Samshvilde is located in the central-eastern part of the Artvin-Bolnisi tectonic zone, which is bordered by the Adjara-Trialeti unit (Santonian-Campanian back-arc) to the north and the Baiburt-Karabakh imbricated unit to the south (Upper Cretaceous fore-arc).

The Artvin-Bolnisi unit is characterised by a Hercynian basement (Pre-Cambrian and Paleozoic granites-gneisses and S-type plagiogranites of the Khrami and Artvin massifs), overlain by Carboniferous volcano-sedimentary rocks (Adamia et al., 2011). The Mesozoic is represented by volcanoclastic rocks of rhyolitic composition (Upper Triassic), overlain by terrigenous clastic sediments and limestones (Lower Jurassic ‘red ammonitic limestones’) and Bajocian tuff-turbidites, lacustrine sandy-clays and lagoonal deposits (Upper Jurassic). Conglomerates, sandstones, sands and shelf carbonate sediments formed during Lower Cretaceous, while calc-alkaline rocks, such as basalts, andesites, dacites and rhyolites formed during the Upper Cretaceous.

Volcanic activity quieted down during the Late Senonian Epoch. From the Palaeocene to the Lower Eocene, shallow-marine limestones and turbiditic terrigenous clastic sediments were deposited; whereupon volcanic activity resumed and a series of calc-alkaline, subalkaline, and alkaline volcanic rocks (andesites, shoshonites, basanites etc.) were deposited until the end of Upper Eocene. In the Oligocene, the formation

of Great Caucasus, the Achara-Trialeti and Lesser Caucasus mountains resulted in sinking of the Georgian and Artvin-Bolnisi massifs and accumulation of molasses in the depressions (until the Miocene). The last period of volcanic activity started in the late Miocene. In both the Lesser Caucasus and the Transcaucasus regions, (a) basaltic, dacitic, rhyolitic and, above all, andesitic lavas characterise the Upper Miocene–Lower Pliocene formations; (b) basaltic (doleritic) lavas predominate in the lower part of the Upper Pliocene–Holocene formations and (c) andesites, andesite-dacites, and dacites represent the last volcanism (Lower Pliocene–Quaternary, maybe the end of Pleistocene). These last rocks (Fig. 3 no. 3) are those upon which Samshvilde was built: a volcanic plateau overlooking the Khrami valley to the south and those of the Chivchava valley to the north.

Geomorphological studies performed by von Suchodoletz et al. (2016) on the Kura River and its tributaries (including the Khrami) showed that rivers channels did not undergo significant migrations during the Quaternary. Moreover, the authors provided some information on the heavy mineral content in a sample from the Khrami River (HM-5 at 41° 28’ 2’’ N, 44° 42’ 12’’ E) which included pyroxene, amphibole, mica, Ti-rich magnetite, tourmaline, sphene, apatite, olivine and epidote.

Georgian clays are poorly investigated. Excluding the clayey deposits studied by Kibaroglu et al. (2009) and Bertolotti and Kuparadze (2018), both of which came from sites distant from Samshvilde; only two samples from the area of interest were investigated, one from Darbazi and the other from Dambludi-Mashavera (Kuparadze et al., 2012; sites nos. 21 and 22 in Figs. 1 and 3). The Darbazi clays are a weathering product of Late Cretaceous acidic volcanites associated with hydrothermally altered acid tuffs, trachytes and subvolcanic bodies of rhyolites. Conversely, Dambludi-Mashavera kaolinite-rich clays occur ‘as sheets on the old granites and alternate with quartz sandstones and conglomerates of Lower Lias’.

Lastly, the Bolnisi district deserves a mention because its gold and copper mines (Popkhadze et al., 2009) were exploited since the pre-history (esp. Sakdrisi, see Hauptmann and Klein, 2009).

### 4. Materials

The samples studied included local raw materials and archaeologically-identified ceramic types of local provenance.

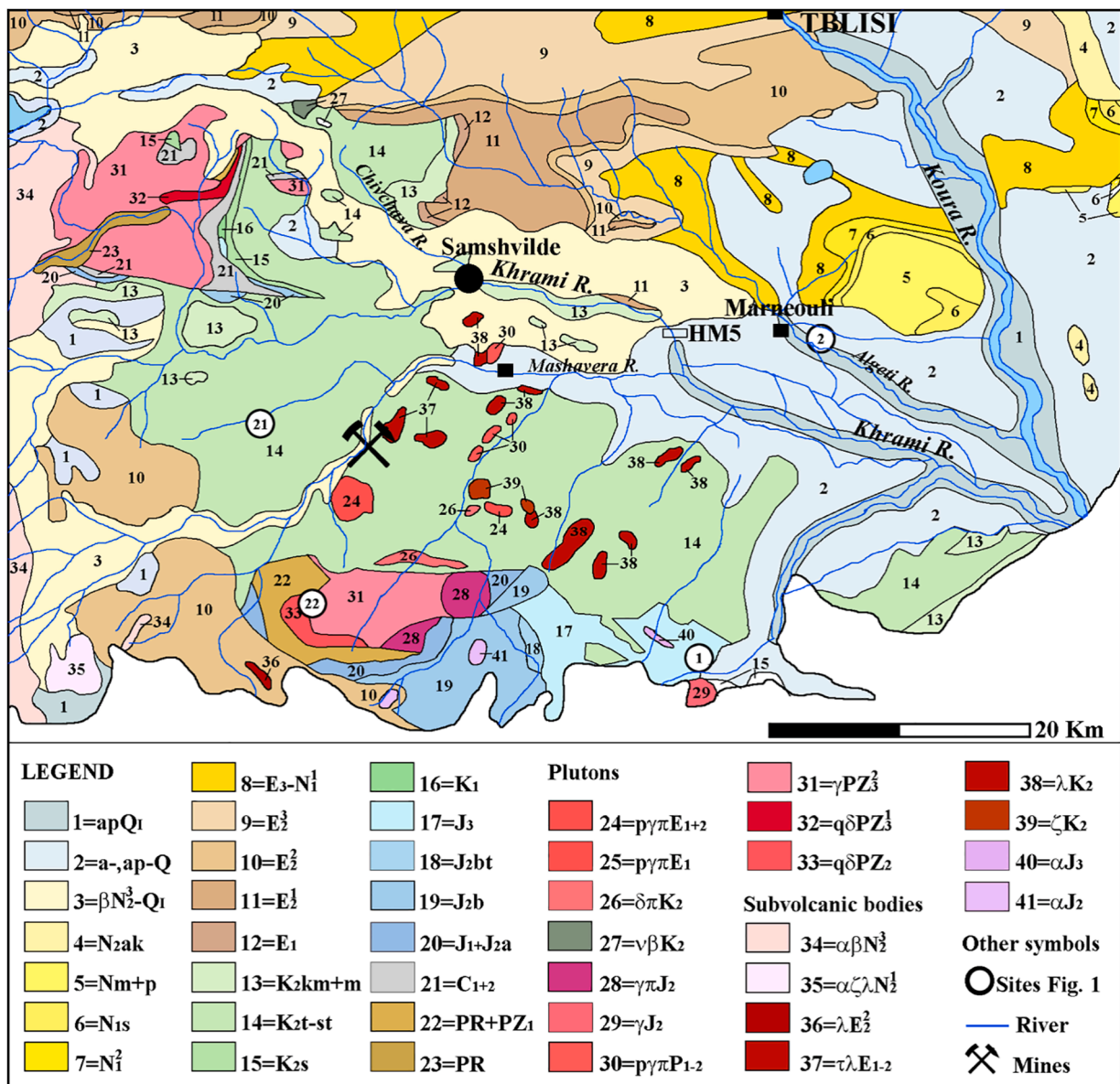


**Fig. 3.** Geological map of the area of Samshvilde (simplified after Gamkrelidze and Gudjabadze 2003). The sites S1 and S2 (circled) correspond to Koda and Kiketi, respectively). The Legend is accurately reported in Appendix 1. The description of nos. 3 and 13 is provided here because they outcrops in the territory of Samshvilde: 3) “Upper Pliocene-Lower Quaternary deposits. Lesser-Caucasian fold system: continental sub alkaline basalts, dolerites and andesite-basalts, andesites, lacustrine conglomerates, sands, sandstones, clays (Tsalka-Akhalkalaki suite)”; 13) “Campanian and Maastrichtian stages. Pelitomorphic limestones and marls, carbonate tuffites with intercalations of tuffs of dacitic composition”.

#### 4.1. Raw materials

Two types of loose sediments were collected from the surroundings of the Samshvilde archaeological site: 1) the samples KR2, representative of the clayey deposits outcropping near the ancient settlement and in contact with alluvial dumps from the Khrami River, and 2) the sample SAM 1, representative of sandy materials possibly used as tempers. Both samples were collected from fresh surfaces after the soil cover was removed.

#### 4.2. Ceramics

Both uncoated Late Bronze Age and glazed medieval ceramics were selected. The rare Bronze Age ceramics were mainly found in the burial cist inside the citadel (trench no. 68) and included jars, jugs, bowls, plates and pots. Overall, these local products are characterised by black

polished surfaces, richly decorated with geometric motifs (e.g. horizontal and vertical lines, zig-zag lines, concentric circles and inscribed notches). Zoomorphic and round-shaped handles are also common features of these black polished ceramics, which are widespread throughout Eastern Georgia. Several examples have been found at Meligela – I (Pitskhelauri, 1973; 2005), Dmanisi (Rezesidze, 2011), Tsiteli Gora (Abramishvili and Abramishvili, 2008), Grakliani Gora (Kvirkvelia and Murvanidze, 2016) and Madnischalis Cemetery (Tushishvili, 1972). The seven samples in this study were selected among pots, bowls and jars of the most representative shapes (Table 1, Fig. 4).

The medieval ceramics included glazed tableware representative of Georgian ceramic typical of the 11th–13th centuries AD. During this period, known as the ‘Golden Age’ in Georgia’s history, the country was unified under a central political government ruled by a monarch. This extended period of political stability favoured the manufacture of objects, especially pottery. Unglazed pottery was produced to a lesser

**Table 1**

Notable information on investigated ceramic samples and raw materials from Samshvilde. In column "Findsite", localization and excavation data are reported (year of discovery in brackets). In column "shape", which portion of the vessel was preserved is indicated in brackets.

<b>Raw materials</b>	<b>Description and findsite</b>				
KR 2	Clay deposit red-brown in colour, Khrami river section. 41°30'23.76" N – 44°32'15.36" E				
SAM 1	Sandy deposit pale-yellow in colour, close to the archaeological site. 41°30'51.48" N – 44°29'15.00" E				
<b>LBA ceramics</b>	<b>Findsite</b>	<b>Ware</b>	<b>Type</b>	<b>Fragment</b>	<b>Chronology</b>
ART 777	Citadel.Trench no. 68 (2018)	Black polished - with horizontal relief stripes	Bowl	Collar	13th-12th BC
ART 786	Citadel. Trench no. 68 (2018)	Fragment of reddish polished - with polished (vertically) and scratched (horizontally) stripes	Pot(?)	Wall	13th-12th BC
ART 791	Citadel.Trench no. 68 (2018)	Black polished with two deep horizontal scratched lines	Bowl	Rim	13th-12th BC
ART 799	Citadel.Trench no. 68 (2018)	Brownish polished	Pot(?)	Wall	13th-12th BC
ART 824	Citadel.Trench no. 68 (2018)	Black burnished ware	Jar	Wall	13th-12th BC
ART 831	Citadel.Trench no. 68 (2018)	Black cooking ware	Jar	Wall	13th-12th BC
ART 850	Citadel.Trench no. 68 (2018)	Black burnished ware with geometric motives	Bowl (?)	Wall	13th-12th BC
<b>MA ceramics</b>	<b>Findsite</b>	<b>Ware</b>	<b>Type</b>	<b>Shape</b>	<b>Chronology</b>
ART 6	Citadel. Trench#69 (2015)	Engobed-Glazed	Bowl	Base foot	12th-13th AD
ART 8Y	Sioni. Trench# N8 (2016)	Engobed-Glazed	Bowl	Wall	12th-13th AD
ART 8G	Sioni. Trench# O17 (2016)	Engobed-Glazed	Bowl	Wall	12th-13th AD
ART 12	Sioni. Trench# O17 (2016)	Engobed-Glazed	Bowl	Wall	12th-13th AD
ART 32	Sioni. Trench# N8 (2016)	Opaque glaze	Bowl	Wall	12th-13th AD
ART 34	Sioni. Trench# N8 (2016)	Engobed-Glazed	Bowl	Wall	12th-13th AD
ART 37	Sioni. Trench# N8 (2016)	Engobed-Glazed	Bowl	Wall	12th-13th AD
ART 42	Sioni. Trench# N8 (2016)	Engobed-Underglaze	Bowl	Wall	11th-12th AD
ART 76	Sioni. Trench# N8 (2016)	Engobed-Glazed	Bowl	Rim	11th-12th AD
ART 94	Sioni. Trench# O17 (2017)	Engobed-Overglaze	Bowl (?)	Rim	11th-13th AD
ART 170	Sioni. Trench# O17 (2017)	Engobed-Glazed	Bowl	Shoulder	12th-13th AD
ART 358	Citadel. Trench#60 (2017)	Engobed-Glazed	Bowl	Wall	11th-12th AD
ART 443	Sioni. Trench# O17 (2017)	Engobed-Underglaze	Bowl	Shoulder	12th-13th AD

extent than glazed pottery. Moreover, the distribution of Georgian glazed pottery crossed international borders and became a characteristic commodity in neighbouring territories such as present-day Azerbaijan, Armenia, Turkey and Iran. Indeed, glazed tableware was common throughout a wide geographical area and the leading centres were located in Iran (especially northern Iran). Several centres, such as Nishapur (Wilkinson, 1961), Mashhad, Tabriz and Ray (Wilkinson, 1973; Grube, 1976) were leading centres; however, Georgia soon developed its own products, while under Iranian influence. Ceramic workshops that produced glazed pottery have been found at Tbilisi (Chilashvili, 1999; Mindorashvili, 2009), Rustavi (Lomtadze, 1988), and Dmanisi (Djaparidze, 1956; Kopaliani, 1996). Thousands of glazed ceramics recovered from excavations of these sites reveal close typological and technical similarity and testify a strong local tradition that lasted until the invasion of the Mongols in the 13th century.

The samples selected for this study were unearthed during the excavations of the citadel walls and the Sioni area. The collections include glazed bowls bearing colourful decorations typical of the 12th and 13th centuries AD (Table 1, Fig. 4).

## 5. Analytical methods

The analytical program examined two different types of material, raw clays and ceramics. The amounts of sample available for analysis varied between a few grams for the ceramics to more than 50 g for clays. Differences in the character and amount of the two types of material required use of different analytical methods (see Supplementary Table S1).

### 5.1. Raw materials

Clayey raw materials were analysed for texture (grain-size

distribution) and composition (mineralogy and chemistry). Approximately 1 kg of each sample was air-dried, gently disaggregated, preliminarily homogenised and quartered. An aliquot of ca. 50 g of the quartered material was further dried in a laboratory oven at 60 °C for 48 h and left in the dryer to cool down to room temperature. This aliquot was mixed with deionised water and dispersed in an ultrasonic bath. The sand fraction was separated according to Stoke's law, dried in the oven (60 °C for 48 h) and weighed. The remaining aqueous suspension containing silt and the clay fractions was disaggregated in the ultrasonic bath. The silt fraction was separated in a centrifuge at 2500 rpm, dried and weighed while the remaining clay fraction (particles < 2 µm) was re-centrifuged at 4000 rpm for 10 min and analysed by XRD and XRF. The XRD analysis was performed using a Bruker D8 Advance X-ray diffractometer (Bruker, Karlsruhe, Germany) with CuK $\alpha$  radiation and a graphite sample monochromator at 40 kV and 40 mA. Scans were collected in the range of 3–60° 2 $\theta$ , a 2° 20 min<sup>-1</sup> scan rate and a 2 s time constant. EVA software (DIFFRAC plus EVA version 11.0. rev. 0) was used to identify mineral phases by comparing experimental patterns with 2005 PDF2 reference patterns. Semi-quantitative estimation was based on peak relative intensity. The XRF analysis was used to quantify major (SiO<sub>2</sub>, TiO<sub>2</sub>, Al<sub>2</sub>O<sub>3</sub>, Fe<sub>2</sub>O<sub>3</sub>, MnO, MgO, CaO, Na<sub>2</sub>O, K<sub>2</sub>O, P<sub>2</sub>O<sub>5</sub>) and trace elements (Ni, Cr, V, La, Ce, Co, Nb, Ba, Y, Sr, Zr, Zn, Rb, Pb). The analyses were performed on pressed pellets containing 5 g of a specimen placed over boric acid (maximum working pressure 25 bar), using a Bruker S8 Tiger WD XRF spectrometer with a rhodium tube of 4 kW intensity and an XRF beam of 34 mm.

### 5.2. Ceramic materials

To prepare the thin sections, ceramic fragments were cut perpendicular to the surface of the object. All thin sections were investigated by OM and SEM. Point analyses (5 µm beam diameter) on single phases and

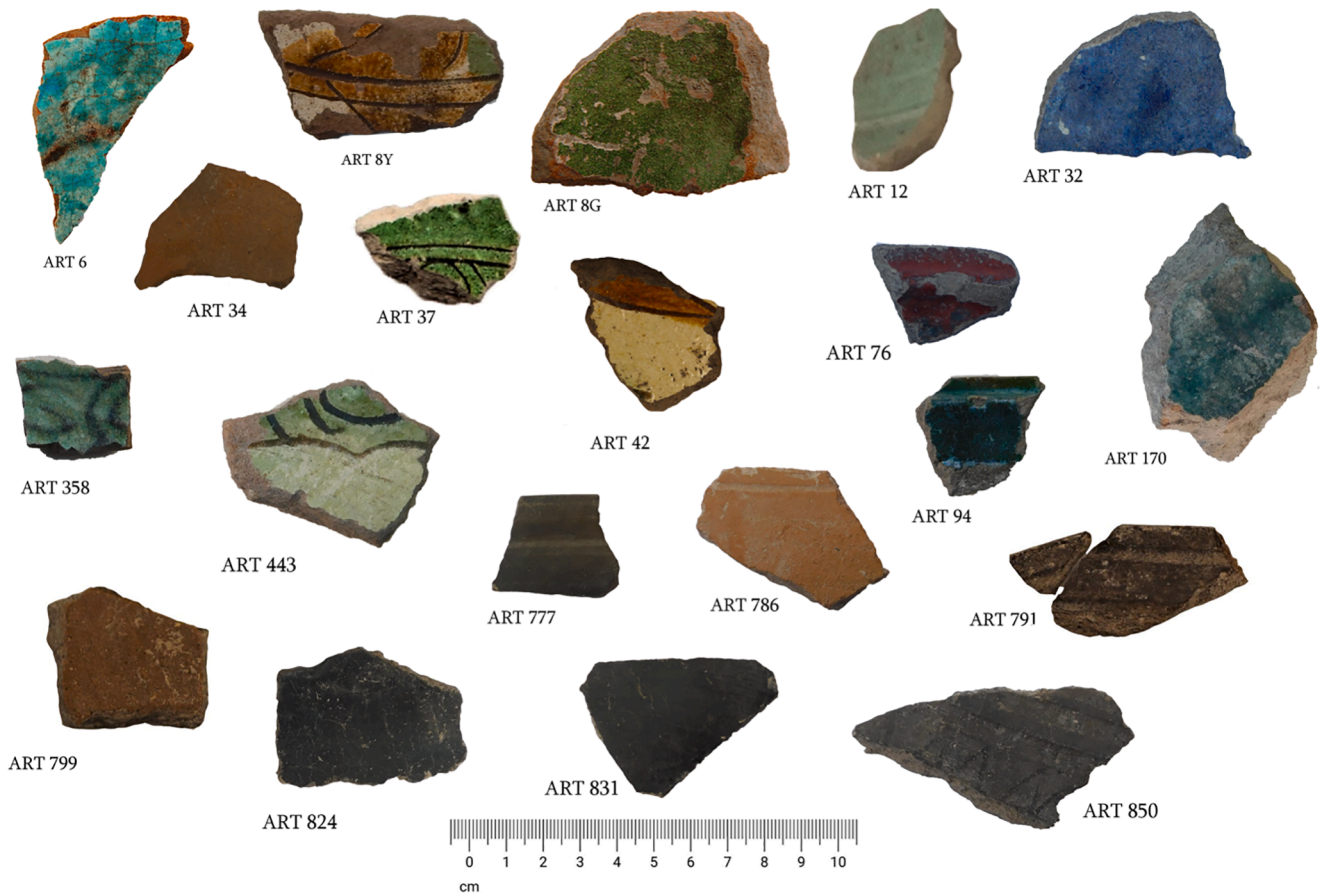


Fig. 4. The investigated collection of prehistoric and medieval ceramics.

square analyses (50/100 μm side) on the matrix were performed. Observations were mostly made using back-scattered electrons (BSE). The instrument used was a Philips XL 30 SEM equipped with an Energy Dispersive Spectrometer (EDAX-DX4), working at 20 kV. A variety of natural silicates, oxides and synthetic materials were used as primary and quality control standards. Micro-chemical analyses were performed on ceramic glazes using an EPMA (JEOL-JXA 8230) coupled with 5 WDS Spectrometers XCE type, equipped with LDE, TAP, LIF and PETJ analysing crystal. Working conditions were: 15 KeV HV, 10nA probe current, 11 mm working distance, ZAF quant correction. A variety of mineral standards (jadeite, olivine, diopside, orthoclase, tugtupite,

pyrite and galena) and pure metals (Fe, Ti, Mn, Cr, Cu, Zn and Sn) were used for calibration and quality control. Bulk chemical analyses were performed by XRF (details are provided above).

6. Results

6.1. Raw materials

Sample KR2 was characterised by similar amounts of silt and clay, which are far more prevalent than the sand fraction (Fig. 5A). Based on Shepard's (1954) ternary diagram, this sample was classified as clayey

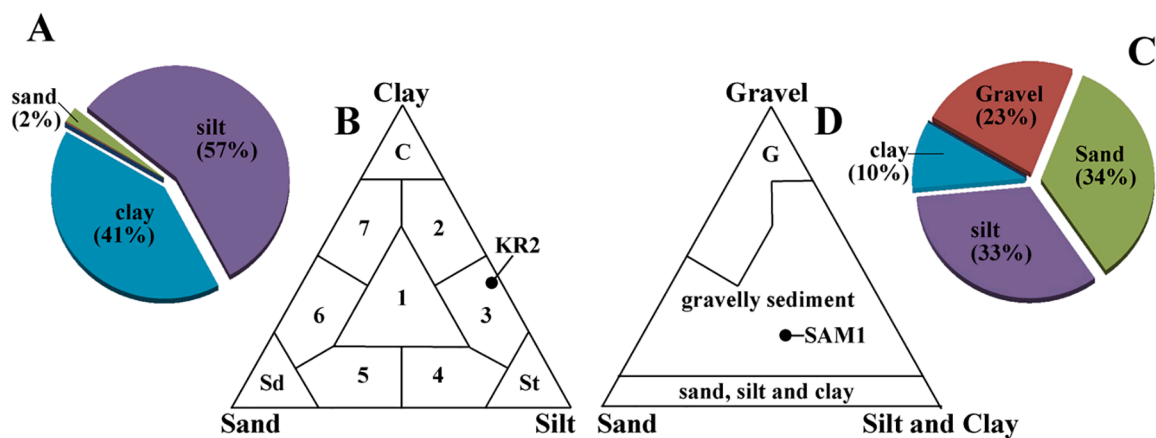


Fig. 5. Grain size analysis on raw materials and the Shepard (1954) classification ternary diagrams for samples KR2 (A-B) and SAM1 (C-D). In ternary B: C = clay; St = silt; Sd = sand; 1) sand, silt and clay; 2) silty clay; 3) clayey silt; 4) sandy silt; 5) silty sand; 6) clayey sand; 7) sandy clay. In ternary D: G = gravel.

silt (Fig. 5B). Calcite and quartz were the main phases, followed by minor amounts of K-feldspar, plagioclase, pyroxene and clay minerals. Hematite showed weak peaks, slightly above the detection limit. The results provided by XRD are consistent with those obtained by XRF. The sum of SiO<sub>2</sub>, CaO and Al<sub>2</sub>O<sub>3</sub> accounted for 85% of the total weight while the other oxides were present in minor amounts.

The sample SAM1 was characterised by a prevalent gravel fraction, followed by the sand, silt and clay fractions (in order of decreasing amounts, Fig. 5C). Based on Shepard's (1954) ternary diagram, this sample was classified as gravelly sediment (Fig. 5D). In the sand fraction, medium (0.25–0.5 mm), fine (0.125–0.25 mm) and very fine (0.06–0.125) grains prevailed over the coarser (greater than 0.5 mm) ones. The mineralogical assemblage of this sample (XRD) included quartz, feldspar, plagioclase and clay minerals (in order of decreasing abundance) and traces of calcite. Accordingly, bulk chemistry showed high SiO<sub>2</sub> content and, to a lesser extent, Al<sub>2</sub>O<sub>3</sub>, together with minor amounts of all other oxides.

## 6.2. Ceramic bodies

All of the ceramic samples showed an unsorted serial texture. Five prehistoric ceramic pieces (ART 791, 799, 824, 831 and 850) and a medieval specimen (ART 94) exhibited a coarse grain-size and a high porosity, while the other samples were characterised by very fine grain-size and a fine porosity. In three of the samples (ART 799, 824 and 850), the pores are elongated and parallel to external surfaces.

The colour is homogeneous in samples ART 12, 32, 94, 358, 443 and 786 and unevenly distributed in the other samples, appearing to be randomly zoned in ART 6, 170, 37, 42, 34, 8y, 8 g, 76, 791 and 799 or zoned from core to surface in ART 777, 824, 831 and 850 (see Supplementary Figure S1).

Micro-textural features were used to discriminate among fine grain-sized samples ART 6, 8G, 8Y, 12, 32, 34, 37, 42, 76, 170, 358, 443, 777 and 786 (i.e. mineral phases mostly ranging between 100 and 150 µm) from coarse grain-sized samples ART 94, 791, 799, 824 and 831 (i.e. mineral phases mostly ranging between 150 and 250 µm). The roundness and sphericity of crystals were highly variable in all samples, except ART 32 that showed high secondary porosity and high degree of sintering.

Based on the results obtained through bulk chemistry (Table 2) and SEM-EDS on the matrices (Table 3), the ceramic collection can be

divided into three main groups (Fig. 6):

- 1) non-carbonatic ceramics (<2.5 wt% CaO and 1.4–3.6 wt% MgO), including 3 prehistoric (ART 786, 799 and 831) and one medieval sample (ART 32);
- 2) intermediate-carbonatic ceramics (6–10 wt% CaO and 3.2–3.9 wt% MgO), including two prehistoric (ART 791 and 824) and six medieval samples (ART 8G, 34, 8Y, 12, 443 and 42, in order of decreasing CaO contents); and
- 3) carbonatic ceramics (11–14 wt% CaO and 3.3–4.7 wt% MgO), including one prehistoric (ART 777) and six medieval samples (ART 37, 6, 76, 170, 358 and 94, in order of decreasing CaO contents).

The MgO content averaged around 3.5 wt%, but was much lower in ART 32 and much higher in ART 94, 358 and 777. The anomalous high lead content revealed in several samples depends on the diffusion of this element from the glaze during firing; therefore, it cannot be considered representative of the composition of the raw material. Lastly, the high iron content in samples ART 799 (Table 3) and ART 831 (Tables 2 and 3) are worth noting.

The results of the mineralogical and petrographic studies performed on the ceramic bodies are presented first and separate from those obtained on glazes. Representative SEM-BSE images of mineral phases and lithic fragments are provided in Supplementary Figs S2–S7. The presence of quartz, K-feldspar and accessory minerals such as Fe and Ti oxides represent common, non-discriminant features. Among the phyllosilicates, white mica was rarely observed in samples ART 170, 791 and 799. Small Mg-Fe chlorites and small biotites (usually showing K loss) were found sporadically in all samples and, in both cases, they rarely exceeded 150 µm in length. More abundant and larger aggregates of chlorite were observed in samples ART 786, 791, 799, 824 and 831.

The relative amount of the different plagioclases were used to identify five groups of ceramic bodies: 1) samples containing the entire series of plagioclases (from albite to anorthite) equally represented (ART 786 and 34); 2) samples with prevalent albite (ART 37 and 791) together with andesine (ART 831) or labradorite (ART 42, 799 and 824) or bytownite (ART 443); 3) samples with prevalent andesine (ART 12 and 94) together with bytownite (ART 170); 4) samples with prevalent labradorite (ART 6, 358, 777) together with bytownite (ART 8Y); and 5) samples with prevalent bytownite (ART 8G and 76).

Among the carbonates, traces of dolomite were found in ART 94,

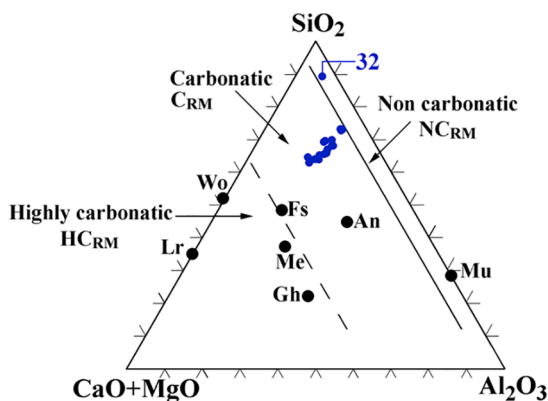
**Table 2**

XRF analyses on raw materials and ceramics. Values normalised to 100% without LOI (although shown in table to provide the reader with a complete information).

Samples	SiO <sub>2</sub>	TiO <sub>2</sub>	Al <sub>2</sub> O <sub>3</sub>	Fe <sub>2</sub> O <sub>3</sub>	MnO	MgO	CaO	Na <sub>2</sub> O	K <sub>2</sub> O	P <sub>2</sub> O <sub>5</sub>	V	Cr	Co	Ni
	wt%	wt%	wt%	wt%	wt%	wt%	wt%	wt%	wt%	wt%	ppm	ppm	ppm	ppm
KR2	51.66	0.75	13.84	6.59	0.12	4.60	19.15	0.73	2.41	0.15	178	89	20	67
SAM1	68.90	0.37	17.51	3.39	0.09	2.18	2.62	2.98	1.88	0.07	57	38	9	21
ART 6	56.66	0.77	15.57	7.58	0.13	3.64	10.90	2.34	2.09	0.29	153	99	22	53
ART 8G	56.90	0.86	16.28	8.50	0.12	4.20	8.13	2.74	2.03	0.16	181	102	27	48
ART 8Y	56.90	0.86	16.18	8.28	0.12	3.99	8.28	2.51	2.45	0.22	175	108	28	54
ART 34	57.04	0.83	16.44	8.28	0.12	4.07	8.29	2.38	2.26	0.29	191	97	27	53
ART 37	57.79	0.80	16.10	8.18	0.12	3.87	8.64	2.10	1.95	0.26	173	107	21	52
ART 42	57.85	0.78	15.83	7.92	0.13	3.81	8.87	2.35	1.94	0.31	158	104	26	55
ART 443	55.99	0.82	15.21	7.82	0.13	3.81	9.71	2.32	1.98	0.31	165	105	25	54
ART 831	60.85	0.96	17.00	9.22	0.14	4.45	3.33	1.67	2.16	0.22	186	146	27	83
Samples	Cu	Zn	As	Rb	Sr	Y	Zr	Nb	Sn	Ba	Pb	La	Ce	LOI
	ppm	ppm	ppm	ppm	ppm	ppm	ppm	ppm	ppm	ppm	ppm	ppm	ppm	
KR2	39	105	–	121	401	32	151	16	22	321	36	17	52	20.7
SAM1	18	59	23	58	454	13	93	8	9	527	18	8	33	8.0
ART 6	87	99	14	69	458	30	158	13	–	460	180	17	44	3.1
ART 8G	149	99	–	69	488	30	157	13	12	433	799	31	47	2.6
ART 8Y	90	99	–	63	530	35	154	11	15	504	2018	25	39	2.0
ART 34	63	95	15	71	448	28	150	14	21	462	150	21	46	3.3
ART 37	78	98	5	66	440	29	157	14	12	461	2090	12	42	2.8
ART 42	74	96	–	70	499	27	145	11	–	563	2096	23	43	3.0
ART 443	123	99	–	83	562	30	173	12	21	522	18,981	18	40	3.0
ART 831	43	111	15	69	273	33	178	13	–	703	24	33	58	7.7

**Table 3**SEM-EDS (wt%) results on the fine matrix. A minimum of five measurements have been taken for each sample, using square analyses of 50/100  $\mu\text{m}$  (side).

		SiO <sub>2</sub>	TiO <sub>2</sub>	Al <sub>2</sub> O <sub>3</sub>	FeO	MnO	MgO	CaO	Na <sub>2</sub> O	K <sub>2</sub> O
ART 32	av.	82.8	0.9	7.0	0.7	0.1	1.4	1.7	4.1	1.3
	sd.	1.1	0.3	0.4	0.1	0.1	0.1	0.2	0.3	0.2
ART 799	av.	63.3	0.9	18.3	7.4	0.1	3.6	2.2	1.4	2.6
	sd.	0.9	0.1	0.5	0.3	0.1	0.3	0.1	0.2	0.0
ART 786	av.	63.1	1.0	18.2	6.1	0.4	3.1	2.3	2.3	3.6
	sd.	1.6	0.2	0.7	0.4	0.2	0.3	0.2	0.4	0.3
ART 831	av.	63.9	1.0	17.8	7.0	0.3	3.4	2.4	1.4	2.8
	sd.	0.8	0.2	0.6	0.3	0.2	0.2	0.4	0.3	0.1
ART 8 g	av.	59.2	1.0	18.1	6.0	0.2	3.9	6.0	3.4	2.2
	sd.	0.6	0.3	0.7	0.6	0.2	0.2	0.9	0.2	0.3
ART 824	av.	60.7	1.1	17.2	6.2	0.3	3.5	6.0	1.6	3.3
	sd.	1.4	0.2	0.5	0.4	0.1	0.2	0.4	0.3	0.2
ART 34	av.	59.3	0.7	17.9	5.8	0.2	3.8	6.4	3.2	2.7
	sd.	1.0	0.1	0.7	0.4	0.1	0.4	0.4	0.3	0.3
ART 8y	av.	58.7	0.7	17.6	5.5	0.3	3.9	7.8	3.1	2.3
	sd.	2.4	0.2	1.0	0.9	0.1	0.7	0.9	0.2	0.3
ART 791	av.	61.0	0.8	15.9	6.2	0.2	3.2	7.9	1.6	3.1
	sd.	1.6	0.1	1.0	0.4	0.2	0.3	1.4	0.3	0.3
ART 12	av.	62.0	0.6	15.8	2.0	0.5	3.7	8.1	6.0	1.4
	sd.	6.0	0.3	1.7	1.1	0.3	0.8	2.1	0.7	0.2
ART 443	av.	58.0	0.6	17.9	5.5	0.2	3.5	9.1	3.0	2.0
	sd.	1.8	0.1	0.9	0.5	0.0	0.5	1.9	0.2	0.3
ART 42	av.	58.1	0.6	17.7	5.2	0.1	3.8	9.7	3.0	1.8
	sd.	1.6	0.3	0.6	0.4	0.1	0.4	1.7	0.2	0.1
ART 37	av.	56.6	1.7	16.5	6.0	0.3	3.3	10.9	2.5	2.0
	sd.	2.7	1.0	1.7	1.4	0.1	0.4	2.2	0.3	0.0
ART 6	av.	56.5	0.8	16.9	5.6	0.3	3.6	11.2	3.0	1.9
	sd.	3.0	0.4	0.6	0.8	0.1	0.4	1.9	0.3	0.5
ART 76	av.	56.5	0.8	17.0	5.3	0.3	3.8	11.3	2.8	1.9
	sd.	1.5	0.2	0.4	0.6	0.1	0.5	1.8	0.3	0.2
ART 170	av.	56.9	0.7	17.3	5.7	0.2	3.6	11.6	2.7	1.1
	sd.	2.9	0.3	1.1	1.1	0.1	0.6	1.5	0.3	0.2
ART 358	av.	55.9	0.9	15.9	5.6	0.3	4.0	11.8	2.9	2.4
	sd.	2.0	0.1	0.9	0.3	0.1	0.0	1.6	0.2	0.2
ART 94	av.	56.7	0.9	14.1	5.0	0.3	4.7	12.7	3.6	1.9
	sd.	2.8	0.1	0.5	0.5	0.1	0.7	1.7	0.9	0.5
ART 777	av.	56.3	0.8	15.4	5.0	0.3	4.2	13.8	2.0	2.1
	sd.	2.0	0.2	0.1	0.5	0.1	0.2	1.5	0.2	0.1

**Fig. 6.** Ternary diagram illustrating the distinction between non-carbonatic, carbonatic and highly carbonatic ceramic bodies.

while calcite was (a) completely absent in samples ART 32, 799, 786 and 831 (either because it was originally absent in the raw materials or transformed by firing); (b) decomposed due to firing in ART 76, 170, 358 and 791; (c) sporadic, without traces of destabilisation in ART 8G, 12, 34, 824 and 850; (d) sporadic, with thin reaction rims in ART 37, 42 and 443; (e) sporadic, but almost decomposed in ART 8Y and 42; (f) frequent, without traces of destabilisation in ART 777; (g) frequent, with evident traces of advanced decomposition in ART 6 and 94.

Among the pyroxenes, the orthopyroxenes were rarely found (enstatite/Mg-pigeonite in ART 6, 8G, 8Y, 34 and 831), and the clinopyroxenes were ubiquitous in all samples, except ART 94 (Fig. 7).

Primary clinopyroxenes showed augitic (ART 6, 8Y, 37, 358, 791, 799, 824 and 831) or augitic and salitic (ART 8G, 12, 34, 76, 170, 443 and 777) or augitic and diopsidic (ART 32, 42 and 786) compositions. Newly formed pyroxenes were found in three samples: 1) ART 94 showed skeletal rods of diopsidic pyroxene confined to the interface between the ceramic body and the coating layer (below 15  $\mu\text{m}$ ); 2) ART 170 showed sporadic Al-rich clinopyroxene rimming former calcite grains; and 3) ART 358 showed sporadic Al-rich clinopyroxene rimming ovate pores (likely formed by decomposition of microfauna).

Amphiboles were ubiquitous, but not as abundant as clinopyroxenes. Brown-coloured clin amphibole, characterised by a Ti-rich hornblende-like composition, were found in samples ART 6, 8Y, 34, 37, 42, 358, 443 831 and 850, while green clin amphiboles, showing a slightly different composition (i.e. no Ti enrichment), were found in samples ART 6, 8G, 34, 94 and 443.

Minor phases were represented by small crystals of olivine, spinel and garnet. Olivine was found in samples ART 6 (Fo<sub>76</sub> with n = 1), 8G (Fo<sub>58-63</sub> with n = 2), 443 (Fo<sub>34</sub> with n = 1), 777 (average of Fo<sub>41</sub> with n = 2), and 791 (Fo<sub>43</sub> with n = 2). Al-rich Cr-spinel and garnet were found in sample ART 76 and in samples ART 6 (Py<sub>26</sub>Gr<sub>38</sub>Sp<sub>35</sub>Al<sub>1</sub> with n = 1) and 791 (Py<sub>10</sub>Gr<sub>53</sub>Sp<sub>37</sub> with n = 1), respectively; however, these last phases were so small in size that their presence in other samples cannot be excluded.

Lastly, abundant accessory and opaque minerals such as Ti-Fe oxides and apatite and, less frequently, titanite, epidote and zircon were common accessory phases.

Lithic fragments were observed in all samples except ART 32. Sedimentary and volcanic rocks are typically present in both fine and coarse ceramics. Sedimentary rocks were more frequent and showed greater

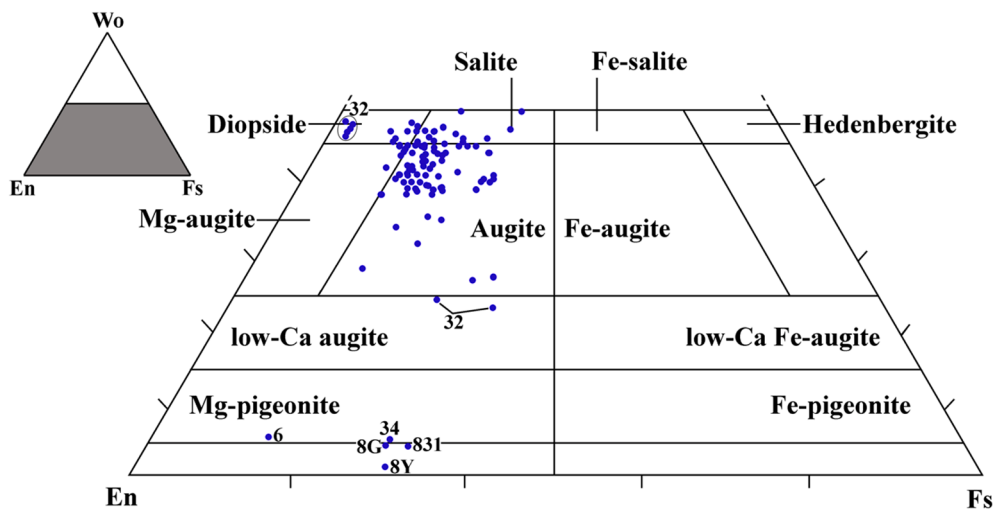


Fig. 7. The chemical composition of the pyroxenes, plotted in the wollastonite (Wo), enstatite (En), ferrosilite (Fs) ternary diagram.

dimensions than the volcanic rocks. They were represented by mudstones, sporadic sandstones and rare ARF (only in ART 42) or chert (only in ART 34). The volcanic rocks showed trachytic, ophitic and intersertal textures and rarely exceed 350  $\mu\text{m}$  in fine grained ceramics. The mineral associations were bytownite + augite (ART 8G and 76), bytownite + augite + olivine (ART 791, 824 and 831), and labradorite + augite (ART 6, 42, 170, 777 and 799), possibly related to basalts and dolerites; andesine + augite (ART 8Y, 12, 42 and 443) related to andesites; quartz + andesine + hornblende (ART 94), possibly related to dacites; and quartz + K-feldspar + augite + chloritised biotite and albite (ART 34), likely related to rhyolites. Other associations, like albite + augite (ART 799) or andesine/labradorite + K-feldspar (ART 777) or quartz + K-feldspar + biotite (ART 358) or K-feldspar + augite (ART 170) were identified and the texture of these fragments suggest that a volcanic origin is more likely than a plutonic or a metamorphic origin. The volcanic glass was clearly identified only in ART 8Y, but it is reasonable to assume that its presence could be more extensive; in fact, the small dimensions and possible transformations due to firing may prevent a precise estimation. Contributions from a metamorphic environment may be hypothesised on the basis of the association orthoamphibole + garnet + chlorite observed in a small clast of ART 6. Lastly, microfossils were identified in ART 12 and hypothetically reconstructed in ART 358.

### 6.3. Ceramic glazes

The composition of the eleven glazes (Fig. 8) was investigated using EMPA (Table 4). The results allowed 4 types of glazes to be distinguished on the basis of alkaline fluxes ( $\text{Na}_2\text{O} + \text{K}_2\text{O}$ ) and lead amounts: 1) alkali glazes composed of silica and alkali oxides (ART 76 and 94); 2) low alkali-low lead glazes with alkaline fluxes and lead content between 5 and 7 wt% and 5 and 15 wt%, respectively (ART 6 and 358); 3) tin-opacified mixed-alkaline lead glaze with tin, lead and alkaline fluxes content of about 4, 25 and 7 wt%, respectively (ART 32); 4) lead glazes with alkaline fluxes below 5 wt% and lead content between 30 and 50 wt% (ART 170, 8Y and 8G); and 5) high lead glazes with alkaline fluxes below 2 wt% and lead content above 50 wt% (ART 443, 37 and 42).

**Alkali glazes** (ART 76, 94). The glaze layer of the carbonatic sample ART 76 exhibited variable thickness but was generally 50–80  $\mu\text{m}$  with composition rich in iron and copper. The glaze was applied over a clear slip that measured 100–180  $\mu\text{m}$  in thickness with high alumina and very low iron content. The carbonatic sample ART 94 shows two layers: a thick (120–180  $\mu\text{m}$ ) blue layer covered by a thin (60–120  $\mu\text{m}$ ) blackish to dark olive-coloured layer. The composition of the two layers was similar, except for the main chromophores with copper in the lower layer and chromium and iron in the upper layer. An EMPA measurement

of a single bright crystal revealed Fe- and Cu-bearing magnesiochromite-like composition (Table 4). Low amounts (below 1 wt%) of lead and tin were measured in both layers. At the interface between the glaze and the ceramic body, newly formed diopsidic pyroxenes (typically 15  $\mu\text{m}$  in size) were frequently observed.

**Low lead-low alkali glaze** (ART 6, 358). The glaze of the carbonatic sample ART 6 contained high levels of copper and was applied over a creamy alumina-rich/iron-poor slip. The glaze of the calcareous sample ART 358 showed a uniform and smooth profile, ranging in thickness between 120 and 200  $\mu\text{m}$  with signs of advanced weathering characterised by notable alkali depletion. Apart from low lead amounts, this glaze also contained high amounts of copper and manganese and very low amounts of tin. Concerning the ceramic body, the thin (20–40  $\mu\text{m}$ ) slip at the interface with the glaze showed higher  $\text{Al}_2\text{O}_3$  and  $\text{Na}_2\text{O}$  content and lower  $\text{SiO}_2$ , FeO, MgO, CaO and  $\text{K}_2\text{O}$  content. Only a few crystals of quartz and, to a lesser extent, K-feldspar (both below 5  $\mu\text{m}$ ) were observed in this slip.

**Tin-opacified mixed-alkaline lead glaze** (ART 32). In sample ART 32, a layered glaze was applied over the ceramic body. The external portion was up to 400  $\mu\text{m}$  thick with numerous, long thin cracks; its composition was homogeneous and contained alkali and lead, with small amounts of tin (ranging between 3.5 and 4.1 wt%) that conferred a white opacity to the glaze (for details on the insolubility of tin particles in lead glaze, see Molera et al., 1999). Conversely, the internal interface was characterised by numerous crystals (up to 80/100  $\mu\text{m}$ ) of quartz embedded in a glassy layer and depleted in Pb and Sn, but enriched in Al and Fe compared to the previous type of glaze.

**Lead glazes** (ART 170, 8G, 8Y). The glaze of the calcareous sample ART 170 showed extensive cracking and heavy alteration. The thickness ranged between 180 and 250  $\mu\text{m}$  and the composition was characterised by low levels of lead (~34 wt%), low levels of alkaline fluxes (below 4 wt%) and high amounts of copper. The slip was slightly thinner (150–220  $\mu\text{m}$ ) than the glaze and highly porous. The composition of the slip was enriched in Al- and Mg compared to that of the glaze and depleted in Al and Mg compared to that of the ceramic body.

The glazes of the intermediate carbonatic samples ART 8G and 8Y were similar in thickness (30–180  $\mu\text{m}$  in 8G, 40–150  $\mu\text{m}$  in 8Y). ART 8G presented a straight smooth profile with small cracks distributed unevenly along the external 20–30  $\mu\text{m}$ . Sample ART 8Y showed an indented profile with many long cracks mostly parallel to the surface with superficial alteration. In both samples, the glaze was applied on a discontinuous and very thin slip. The initial formation stage of the ‘digestion’ interface denotes a low firing temperature (for details, see the digestion process illustrated by Molera et al., 2001). Different colours are caused by the presence of copper (green) and iron (yellow). In

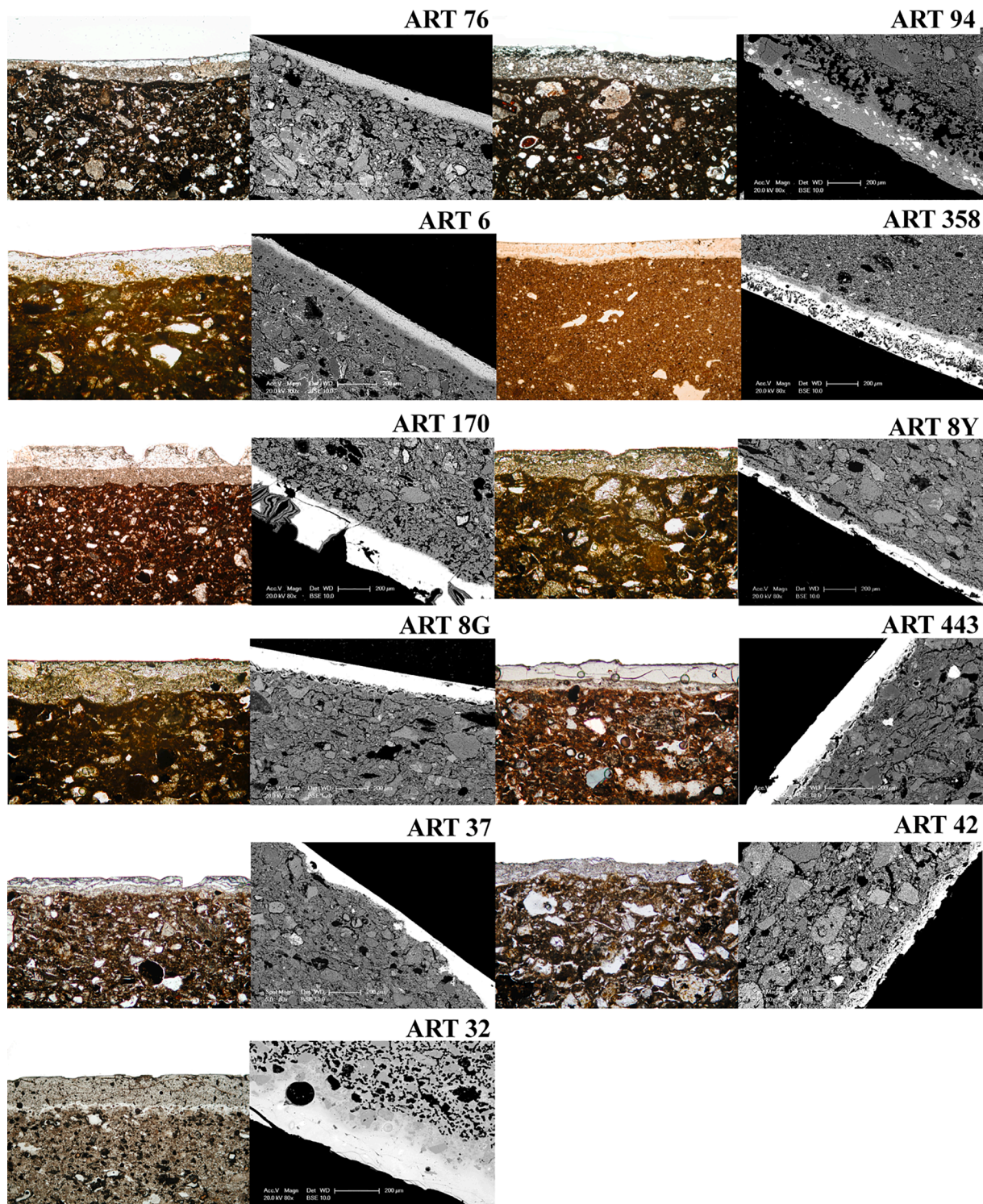


Fig. 8. OM and SEM-BSE images of slips and glazes.

sample ART 8G, the association of high Zn and high Cu content was notable.

*High lead glazes* (ART 443, 37, 42). The glaze of the intermediate carbonatic sample ART 443 showed a uniform and smooth profile of variable thickness (80–140  $\mu\text{m}$ ) and a composition characterised by small amounts of copper and iron. The internal slip varied in thickness (20–80  $\mu\text{m}$ ) and its Fe-rich composition was partially contaminated by lead from the upper glaze. The glaze of the carbonatic sample ART 37 varied in thickness (50–250  $\mu\text{m}$ ) and displayed a linear profile. The

chromophore with the highest contents was copper, that is likely associated with the relatively high contents of zinc and tin (each both below 0.5 wt%). The slip was very thin (20–60  $\mu\text{m}$ ) and Fe-rich, but as also observed in ART 443, its composition was contaminated by the upper lead glaze. Lastly, the glaze of the intermediate carbonatic sample ART 42 was poorly preserved and showed variable thickness (40–90  $\mu\text{m}$ ). The slip showed an irregular profile due to poor smoothing of the ceramic body.

**Table 4**

The composition of glazes (Gl) and slips (Sl) measured by EMPA. Average (n = ) and standard deviation (sd) values. [The slip of samples ART76 and 170 have been analysed by SEM-EDS]

ART	Colour	Area	n	SiO <sub>2</sub>	TiO <sub>2</sub>	Al <sub>2</sub> O <sub>3</sub>	Cr <sub>2</sub> O <sub>3</sub>	FeO	MnO	MgO	CaO	Na <sub>2</sub> O	K <sub>2</sub> O	Cl	SO <sub>3</sub>	ZnO	SnO <sub>2</sub>	CuO	PbO	Total	
<b>Alkali glazes</b>																					
76	R	Gl	3	71.88	0.25	6.04	0.00	2.69	0.12	2.37	4.58	7.82	1.90	0.41	0.18	0.05	0.03	1.65	0.02	99.9	
			sd	1.84	0.06	1.50	0.00	1.44	0.03	0.44	0.72	0.54	0.17	0.07	0.06	0.03	0.04	0.19	0.04		
94	Bk	Gl	3	57.8	0.1	25.7	0.00	0.6	0.1	1.5	0.8	5.9	0.7	0.00	0.00	0.00	0.00	0.00	0.00	100	
			sd	82.55	0.10	4.68	1.27	1.81	0.01	1.96	1.25	3.34	2.00	0.07	0.06	0.01	0.13	0.67	0.08	99.9	
	Bl	Gl	4	78.18	0.21	4.65	0.05	0.36	0.06	1.24	1.90	5.92	2.39	0.06	0.08	0.02	0.45	4.23	0.22	99.9	
			sd	1.30	0.09	1.34	0.04	0.11	0.02	0.22	0.31	0.15	0.11	0.02	0.05	0.02	0.09	1.40	0.13		
<b>Low-lead-(low) alkali glazes</b>																					
6	Tq	Gl	4	75.73	0.20	3.16	0.01	0.70	0.04	1.22	3.94	5.63	1.56	0.07	0.17	0.06	0.01	2.10	5.40	100.0	
			sd	0.38	0.13	0.34	0.02	0.11	0.02	0.03	0.12	0.14	0.14	0.14	0.02	0.09	0.09	0.01	0.06	0.23	
358	G	Gl	1	65.52	0.09	23.01	0.02	0.30	0.01	0.61	0.00	7.18	3.18	0.03	0.05	0.00	0.00	0.00	0.00	100.0	
			sd	64.32	0.20	3.06	0.02	1.02	2.01	1.53	5.58	3.20	2.04	0.26	0.00	0.05	0.29	2.02	14.41	100.0	
	Sl	Sl	3	64.32	0.20	3.06	0.02	1.02	2.01	1.53	5.58	3.20	2.04	0.26	0.00	0.05	0.29	2.02	14.41	100.0	
			sd	1.51	0.10	1.10	0.02	0.61	0.13	0.19	1.41	0.29	0.08	0.13	0.00	0.06	0.09	0.40	1.16		
170	G	Gl	4	55.39	0.06	2.14	0.01	0.47	0.02	0.66	1.16	2.99	0.65	0.20	0.00	0.00	0.24	2.29	33.73	100.0	
			sd	1.41	0.06	1.13	0.01	0.07	0.01	0.03	0.17	0.18	0.18	0.02	0.04	0.00	0.00	0.28	0.31	2.10	
8Y	Y	Gl	1	77.1	0.3	13.4	0.00	0.92	0.01	1.89	1.2	2.1	2.6	0.00	0.00	0.00	0.00	0.00	0.00	100.0	
			sd	36.54	0.39	8.25	0.01	4.60	0.05	1.47	4.36	1.03	1.51	0.03	0.00	0.02	0.03	0.22	41.49	100.0	
8G	G	Gl	3	38.25	0.27	5.44	0.01	0.79	0.01	0.64	2.88	0.56	0.99	0.03	0.00	0.14	0.06	1.99	47.94	99.9	
			sd	0.94	0.03	0.45	0.02	0.09	0.02	0.08	0.13	0.05	0.09	0.02	0.00	0.04	0.04	0.15	1.18		
<b>High lead glazes</b>																					
443	Tr	Gl	5	31.20	0.19	5.71	0.01	0.89	0.02	0.57	1.71	0.41	1.04	0.01	0.00	0.03	0.03	0.25	57.92	100.0	
			sd	0.57	0.10	0.09	0.02	0.06	0.01	0.02	0.06	0.03	0.03	0.02	0.01	0.00	0.05	0.03	0.04	0.43	
37	G	Gl	1	45.98	0.21	16.02	0.00	1.39	0.05	1.64	4.37	1.25	3.88	0.00	0.00	0.07	0.00	0.09	25.06	100.0	
			sd	24.11	0.09	6.40	0.00	1.02	0.05	0.60	2.83	0.45	0.86	0.02	0.00	0.20	0.41	1.64	61.33	100.0	
42	Y	Gl	3	6.60	0.08	0.26	0.00	0.25	0.03	0.06	0.17	0.01	0.07	0.02	0.00	0.17	0.01	0.25	0.49		
			sd	53.49	0.09	15.33	0.03	0.70	0.00	0.30	1.01	2.10	6.33	0.02	0.00	0.03	0.03	0.81	19.74	100.0	
32	Bl	Gl ext	4	24.14	0.09	6.79	0.02	0.45	0.02	0.58	1.40	0.33	1.01	0.01	0.00	0.01	0.01	0.10	65.05	100.0	
			sd	0.34	0.07	0.25	0.01	0.11	0.01	0.05	0.05	0.02	0.23	0.01	0.00	0.01	0.01	0.04	0.41		
94	Bright crystals	Gl int	5	55.93	0.07	1.59	0.01	0.55	0.02	2.06	3.55	5.76	1.16	0.69	0.00	0.04	3.74	0.03	24.80	100.0	
			sd	0.66	0.06	0.06	0.02	0.04	0.02	0.06	0.14	0.06	0.03	0.03	0.03	0.00	0.05	0.26	0.03	0.72	
94	Bright crystals	Gl int	1	78.10	0.32	9.45	0.03	1.13	0.00	0.90	0.65	4.76	2.50	0.44	0.10	0.02	0.01	0.00	1.60	99.9	
			sd	6.8	0.2	9.1	56.1	7.1	0.2	12.7	0.1	0.3	0.1	0.0	0.0	0.0	0.0	0.0	7.3	0.0	100.0

[Colours abbreviations: Bl = blue; Bk = blackish dark olive; G = green; l. = light; R = red; Tr = transparent; Tq = turquoise; Y = yellow; W = white.]

## 7. Discussion

The main microstructural, chemical, mineralogical and petrographic features described in Section 6 correlated with different raw materials and different technologies. Grain size helped us distinguish between fine wares and coarse wares and likely addresses two different raw materials rather than a levigation process because they are both poorly sorted. If the starting assumption is correct and these are locally-made products, this distinction could correspond to diversified use of KR2-type clays, which may have been exclusively for fine wares and mixed with SAM1-type deposits for coarse wares. The content of carbonates provides a further distinctive criterion because no temper made of spatic calcite was observed. On this basis, non carbonatic, intermediate carbonatic and carbonatic ceramics should have come from different raw materials; however, considering the typically high compositional variability of alluvial sediments, this reconstruction needs to be taken with caution. Combining grain size with the degree of carbonates in the ceramic bodies, it was possible to distinguish fine wares from coarse wares (Table 5). On the same basis, a technological difference was inferred, which combined the degree of sintering of the matrix with the degree of transformation of calcite crystals. The general picture is complicated for fine ceramics because the maximum temperatures obtained during firing were low (i.e., low degree of sintering and unreacted calcite), medium (i.e., low to medium degree of sintering with calcite transformation in progress) and high (i.e., medium to high degree of sintering and decomposed calcite), regardless of the amount of carbonates. On the other hand, coarse wares were fired at low temperatures, except for the medieval sample ART 94. Given that the temperature range of calcite destabilisation and decomposition is 650°-900 °C (Gliozzo, 2020b), most samples were fired at maximum temperatures included in this range. However, a few samples (ART 94, 170, 358 and 32) must have reached maximum temperatures above 850 °C since they showed a high sintering degree, no calcite and newly formed phases such as diopside and Al-rich clinopyroxenes.

Further information on the technology and use of these ceramics was obtained from the observation of colour distribution and surface treatments. Samples ART 824 and 850 bore clear evidence of burnishing, while samples ART 777 and 831 were used for cooking food over the fire. The uneven distribution of colour in samples ART 6, 170, 37, 42, 34, 8y, 8 g, 76 and 791 supports changing redox conditions during firing; however, compositional differences were not observed between brighter and darker areas. Conversely, the homogeneous colour distribution of the other samples (ART 12, 32 and 358) suggests that a constant level of oxygen fugacity was maintained during firing or that an oxidising atmosphere was maintained for a sufficient time during the last stage of the process.

The composition of both plagioclases and primary pyroxenes, combined with mineralogical assemblages observed in lithic fragments, provide a further clue as to where local materials were obtained. For example, among plagioclases, sodic terms were nearly absent while calcic terms were ubiquitous and frequently combined with augitic clinopyroxenes, either as isolated crystals or as lithic fragments. The augitic clinopyroxenes suggest a volcanic environment represented by dolerites and andesites, although basalts, dacites and rhyolites can be also present. This evidence is consistent with the lithology of the area (see Section 3 Geological Setting) and supports the starting assumptions that claims these ceramics are of local origin. However, several features suggest multiple production sites or multiple raw material supply sites, including the partially different nature of lithic fragments in sample ART 34, the presence of olivine in a few samples (ART 777, 6, 8G and 443), the abundant microfauna of sample ART 12 and traces of former microfossils in ART 358.

As far as glazes are concerned, while the results obtained for the lead glazes easily fit within the broad framework offered by these types of ceramics, some interesting features emerged for the alkali glazes, the low alkali-low lead glazes and the tin glaze.

The alkali glazes (ART 76 and 94) were applied on carbonatic bodies, but the grain size was fine in ART 76 and coarse in ART 94. The use of a slip combined with an alkali glaze was not frequent but documented, for example, in the Islamic turquoise and the blue 'coloured monochrome-glazed shards' from Jordan investigated by al-Saad (2002) and the 12th-13th century CE alkaline glazes from Termez (Molera et al., 2020). Similarly, the overglaze technique demonstrated in ART 94 was identified in green and black 9th-10th century pottery from al-Andalus (Molera et al., 2009, 2013; Salinas, 2018).

Continuing the comparison, the fluxing agents (soda and potash) and the alkaline earths (lime and magnesia) made a minor contribution to the glaze recipe in both samples (Table 5). These amounts testify to the use of plant ash to lower the melting temperature of the silica-rich glaze, but made it difficult to compare these specimens with other alkaline glazes. The latter, in fact, were generally characterised by higher alkali content, for example, the sum of Na<sub>2</sub>O and K<sub>2</sub>O ranged between 16.7 and 19.3 wt% in Islamic pottery from Dohaleh in Jordan (al-Saad, 2002), between 11 and 16.7 wt% in the 12th-17th century CE Termez ceramics (Molera et al., 2020), between 14 and 24 wt% and between 15 and 20 wt% in the 11th-13th century Syrian and Iranian alkali glazes, respectively (Mason et al., 2001) or between 12.4 and 18.1 wt% in the 1st-7th century Sasanian glazed pottery from Veh Ardašir (Pace et al., 2008).

As for colouring agents, the comparison was straightforward for copper (i.e., a well-known and widely used chromophore), responsible for both the red (ART 76) and the blue (ART 94) colours. The use of chromium was more limited and likely began in a later period as exemplified by 9th-10th century lead glazes from Nishapur (Holakooei et al., 2019) and by 12th century black alkali-glazed from Iran (Mason et al., 2001).

The low lead (low) alkali glazes (ART 6, 358) were applied over an Al-rich slip, instead of a carbonatic ceramic body. The particularity is the composition of the glaze that does not match with the compositional range provided by Tite et al. (1998) for the low lead-alkali type (2/10 wt % PbO, ~14 wt% Na<sub>2</sub>O + K<sub>2</sub>O, ~10 wt% MgO + CaO and 2 wt% Al<sub>2</sub>O<sub>3</sub>). ART 6 contained fewer fluxing agents (~7 wt%) and alkaline earths (~6 wt%), while ART 358 showed higher amounts of PbO and lower amounts of fluxes (~5 wt%) and alkaline earths (~7 wt%). Overall, these compositions find small comparison; for example, ART 6 can be compared with the Early Islamic Turquoise-glaze wares from Iraq investigated by Mason and Tite (1997) which showed 1/3 wt% PbO, 9/20 wt% Na<sub>2</sub>O + K<sub>2</sub>O, 5/10 wt% MgO + CaO and 3/5 wt% Al<sub>2</sub>O<sub>3</sub>, while ART 358 finds a close comparison with green-glazed wares from Uzbekistan investigated by Henshaw (2010) (e.g. sample Tashkent 4). Colouring agents such as manganese (black stripes in ART 358) and copper (turquoise and green) were commonly used.

The composition of tin-opacified mixed-alkaline lead glaze (ART 32) was common (see al-Saad, 2002; Tite et al., 2008; Gulmini et al., 2013, for comparison) but this specimen was unique because the glaze was applied over a non carbonatic high-fired ceramic body. A few samples found at Termez in Uzbekistan (samples TA1 and TS1; Molera et al., 2020) showed a similar composition but the glaze was applied over a carbonatic ceramic body. In this regard, it is interesting to note that the reference materials are believed to be of Iraqi or Iranian or Syrian or, less likely, Egyptian provenance (Martínez Ferreras et al., 2019).

The lead glazes described herein exemplified techniques and compositions considered typical. Numerous similar examples are provided for pottery and tiles from Cyprus (Ting et al., 2019a), Jordan (al-Saad, 2002; Ting et al., 2019b), Egypt, the Levant, Mesopotamia, Iran and Central Asia (Matin, 2018 with tin), Afghanistan (Gulmini et al., 2013), Uzbekistan (Henshaw, 2010, Molera et al., 2020), and central and western European countries such as Italy, Spain, Portugal and the UK (Tite et al., 1998; Coentro et al., 2017). The ceramic bodies are fine grained and intermediate-carbonatic to carbonatic in composition. The lead content in the glazes ranged between 34 and 65 wt% and the chromophores were represented by copper (turquoise in ART 170, green

**Table 5**  
Results summary. Microstructural descriptions have been made on a comparative basis and they are relative to the examined context only. Detailed compositional data are provided in Tables 2-4 and Supplementary Table S2.

Period	Sample	Micro-structural features					Ceramic body										Glaze						
		Grain size	Roundness	Sphericity	Porosity	Sintering	Chemical c.	Calcite	Plagioclase	P. Cpx	N.F. Cpx	Cam	Minor	Lithic fr.	Microfauna	Colour	Slip	Type	Na <sub>2</sub> O + K <sub>2</sub> O	CaO + MgO	Pb	Sn	Chromop.
<i>Fine</i>																							
LBA	ART 777	F	A/S	L/M	Hf	L	C <sub>RM</sub>	Fu	La	Au/Sa	-	-	Ol	Ba-Do, V	-	-	-	-	-	-	-	-	
MA	ART 6	F	S	L/M	Hf	L	C <sub>RM</sub>	Fr	La	Au	-	B-G	Ol-Grt	Ba-Do; M?	-	T	X	IA-IPb	7	5	5	-	Cu
MA	ART 37	F	A/S	L	Hf	M	C <sub>RM</sub>	Sr	Ab	Au	-	B	-	V	-	G	X	HPb	1	3	61	-	Cu
MA	ART 76	F	S/R	M/H	Hf	M	C <sub>RM</sub>	D	By	Au/Sa	-	-	Cr	Ba-Do	-	R	X	A	10	7	-	-	Cu (Fe)
MA	ART 170	F	S/R	M/H	Hf	H	C <sub>RM</sub>	D	An, By	Au/Sa	Al	-	-	Ba-Do, V	-	G	X	Pb	4	2	34	-	Cu
MA	ART 358	F	S/R	L/M	Hf	H	C <sub>RM</sub>	D	La	Au	Al	B	-	V	?	G	X	IA-IPb	5	7	14	-	Cu-Mn
MA	ART 8Y	F	S	M	Hf	M	IC <sub>RM</sub>	Sr	La, By	Au	-	B	-	An; G	-	Y	X	Pb	3	6	41	-	Fe
MA	ART 8G	F	A/S	L/M	Hf	M	IC <sub>RM</sub>	Su	By	Au/Sa	-	G	Ol	Ba-Do	-	G	X	Pb	2	4	48	-	Cu
MA	ART 12	F	A/S	H	Hf	L	IC <sub>RM</sub>	Su	An	Au/Sa	-	-	-	An	µF	G	X	n.a.	n.a.	n.a.	n.a.	n.a.	n.a.
MA	ART 34	F	A/S	L/M	Hf	L	IC <sub>RM</sub>	Su	Ab/An	Au/Sa	-	B-G	-	Ry	-	-	X	n.a.	n.a.	n.a.	n.a.	n.a.	n.a.
MA	ART 42	F	A/S	L/H	Hf	M	IC <sub>RM</sub>	Sr	Ab, La	Au/Di	-	B	-	Ba-Do, An	-	Y	X	HPb	1	2	65	-	-
MA	ART 443	F	A/S	L/H	Hf	M	IC <sub>RM</sub>	Sr	Ab, By	Au/Sa	-	B-G	Ol	An	-	Tr.	X	HPb	1	2	58	-	Fe
MA	ART 32	F	A/S	-	Hs	vH	NC <sub>RM</sub>	-	-	Au/Di	-	-	-	-	-	Bl	-	Sn	7	2	25	4	-
LBA	ART 786	F	A/S	L/M	Hf	L	NC <sub>RM</sub>	-	Ab/An	Au/Di	-	-	-	V	-	-	-	-	-	-	-	-	-
<i>Coarse</i>																							
MA	ART 94	C	A/S	L/M	Hc	M	C <sub>RM</sub>	Fr	An	-	Di	G	-	Da	-	Bl-Bk	X	A	5	3	-	-	Cu-Cr
LBA	ART 791	C	A/S	L/M	Hc	L	IC <sub>RM</sub>	D	Ab	Au	-	-	Ol-Grt	Ba-Do	-	-	-	-	-	-	-	-	-
LBA	ART 824	C	A/R	L/H	Hc	L	IC <sub>RM</sub>	Su	Ab, La	Au	-	-	-	Ba-Do	-	-	-	-	-	-	-	-	-
LBA	ART 799	C	A/S	L/M	Hc	L	NC <sub>RM</sub>	-	Ab, La	Au	-	-	-	Ba-Do, V	-	-	-	-	-	-	-	-	-
LBA	ART 831	C	A/R	L/H	Hc	L	NC <sub>RM</sub>	-	Ab, An	Au	-	B	-	Ba-Do	-	-	-	-	-	-	-	-	-
LBA	ART 850	C	A/R	L/H	Hc	L	n.a.	Su	n.a.	n.a.	-	B	-	V	-	-	-	-	-	-	-	-	-

ABBREVIATIONS. **Microstructural features** - Grain size: F = Fine (with mineralogical phases averagely ranging between 100 and 150 µm); C = coarse (with mineralogical phases averagely ranging between 150 and 250 µm). Clasts roundness: A = angular, S = subrounded, R = rounded. Clasts sphericity: L = low, M = medium, H = high. Porosity: Hf = high fine; Hc = high coarse; Hs = extensive secondary. Sintering degree: l = low, M = medium, H = high. Chemical composition (c.): NC<sub>RM</sub> = non carbonatic raw material; IC<sub>RM</sub> = intermediate-carbonatic raw material; C<sub>RM</sub> = carbonatic raw material. **Mineralogical composition** - Prevalent plagioclases: Ab = albite; Ol = oligoclase; An = andesine; La = labradorite; By = Bytownite; An = anorthite. Calcite: D = decomposed; Su = sporadic and apparently unreacted; Ss = sporadic and slightly reacted; Sr = sporadic and reacted; Fu = frequent and unreacted; Fu = frequent and reacted. Primary (P) and newly formed (N.F.) clinopyroxenes (Cpx): Au = augite; Sa = salite; Di = diopside; Al = Al-rich clinopyroxene. Clinoamphiboles (Cam): B = brown hornblende; G = green hornblende. Minor (phases): Ol = olivine; Cr = Al-rich Cr spinel; Grt = garnet. Lithic fragments: Ba = basalt; Do = dolerite; An = andesite; Da = dacite; Ry = Rhyolite; V = generic volcanic; G = glass; M = metamorphic. Microfauna: µF = frequent; ? = hypothetically present before firing. **Glazes** - Colour: Bl = blue; Bk = blackish dark olive; G = green; O = orange; R = red; T = turquoise; Tr. = transparent; Y = yellow; W = white. Glaze type: A = alkali glaze; IA-IPb = low alkali-low lead glaze; Sn = Tin-opacified mixed-alkaline lead glaze. In all fields n.a. = not analysed.

in ART 8G and 37) and iron (yellow in ART 8Y).

Lastly, in all samples (except for ART 42 and 170), the presence of low amounts of tin and/or zinc cannot be clearly related to a deliberate addition but may result from the introduction of brass or gunmetal as a source of copper.

## 8. Conclusions

Returning to the history of archaeometric studies outlined at the beginning of this paper, it is clear that the research performed to date can be considered preliminary, particularly in consideration of the fact that it is mostly focused on the prehistoric period. In this framework, research on Samshvilde pottery has presented, for the first time, the extreme variety and complexity of the medieval repertoire.

The analytical results describe a complex and heterogeneous ceramic collection, from whichever point of view from it is observed. While such an outcome was expected as a consequence of a heterogeneous sample selection, several unexpected findings signal the need for additional studies and provide guidance for future research.

For example, the glazes proved to be compositionally different; in fact, their composition was classified under the known types of alkali, low alkali – low lead, lead, high lead and tin-opacified mixed-alkaline lead glazes. The ground for comparison was wide for lead glazes and spanned from the Near East to the western Mediterranean basin. Conversely, the composition and technique of alkali and low alkali – low lead glazes partially differed from those reported in the literature. Further particularities were found in relation to (a) the application of an alkaline glaze over a coarseware (ART 94) and (b) the application of a tin-opacified mixed-alkaline lead glaze over a non carbonatic ceramic body. In all cases, the differences (or the particularities) were never so sharp as to claim new productions but sufficient to underscore that these poorly known contexts contribute to the history of glazed ceramics, especially in the medieval period.

As for the geographic localisation, the lack of reference groups weighs heavily on the conclusions we can draw. While the territory is unique on a regional scale, the results do not suggest that Samshvilde or other sites in the vicinity were the only supply or production centres. The mineralogical assemblages and lithic fragments indicate a volcanic environment, but the extent of this environment cannot be further delimited. Assuming that prehistoric ceramics were not transported over long distances, the similarity of the petrographic results obtained for the prehistoric and the medieval pottery may indicate a limited geographic area; however, other features such as the carbonate content, the presence/absence of specific phases (e.g., plagioclases and olivine) or microfauna, together with the compositional and technological differences observed in the glazes, seem to indicate multiple sources of raw materials and multiple production centres. Some glazes, for example ART 32, suggest a provenance from other Near Eastern countries such as Iraq.

## CRedit authorship contribution statement

**L. Randazzo:** Formal analysis, Investigation, Writing - original draft, Writing - review & editing. **E. Gliozzo:** Formal analysis, Investigation, Writing - original draft, Writing - review & editing. **M. Ricca:** Formal analysis, Investigation. **N. Rovella:** Formal analysis, Investigation. **D. Berikashvili:** Investigation, Writing - original draft. **M.F. La Russa:** Conceptualization, Supervision.

## Acknowledgments

This research did not receive any specific grant from funding agencies in the public, commercial, or not-for-profit sectors. The authors would like to thank the anonymous reviewers for their insightful suggestions and careful reading of the manuscript.

## Appendix A. Supplementary data

Supplementary data to this article can be found online at <https://doi.org/10.1016/j.jasrep.2020.102581>.

## References

- Abramishvili, R., Abramishvili, M., 2008. Late Bronze Age Barrows at Tselgori, Archaeology in Southern Caucasus: Perspectives from Georgia, *Ancient Near Eastern Studies, Supplement XIX*, edited by Sagona and M. Abramishvili, Leuven-Paris Dudley.
- Adamia, S., Zakariadze, G., Chkhotua, T., Sadradze, N., Tsereteli, N., Chabukiani, A., Gventsadze, A., 2011. Geology of the caucasus: a review. *Turk. J. Earth Sci.* 20, 489–544.
- al-Saad, Z. 2002. Chemical composition and manufacturing technology of a collection of various types of Islamic glazes excavated from Jordan. *Journal of Archaeological Science* 29: 803-810. DOI: 0.1006/jasc.2000.0576.
- Amadori, M.L., Del Vais, C., Fermo, P., Pallante, P., 2017. Archaeometric researches on the provenance of Mediterranean Archaic Phoenician and Punic pottery. *Environ. Sci. Pollut. Res.* 24 (16), 13921–13949. <https://doi.org/10.1007/s11356-016-7065-7>.
- Badalyan, R.S., Chataigner, C., Kohl, P. 2004. Trans-Caucasian obsidian: the exploitation of the sources and their distribution. In: A. Sagona (ed.), A view from the highlands. *Archaeological studies in honour of C. Burney, Ancient Near Eastern Studies* 12: 437–65. Leuven: Peeters.
- Berikashvili, D., Coupal, I. 2018. The First Evidence of Burials from Samshvilde A Preliminary Archaeological and Bioarchaeological Study. *Caucasus Journal of Social Sciences*. Vol. 11. The Publishing House of the University of Georgia. Tbilisi, pp. 31-49. <https://www.ug.edu.ge/storage/journals/January2020/dVSSYQjKu05dWbZyNyw7.pdf>.
- Berikashvili D., Coupal Is., Tvaladze Sh., Kvakhadze L. 2019. The results of archaeological excavations in Samshvilde in 2019. Tbilisi.
- Berikashvili, D., Coupal, I. 2019. Recently Discovered Late Bronze Period Burial from Samshvilde Citadel. *Archaeology*, vol.3. The publishing house of the University of Georgia. Tbilisi, pp. 120-136.
- Berikashvili D., Pataridze M. 2019. Samshvilde Hoard. Tbilisi.
- Bertolotti, G.P., Kuparadze, D., 2018. White Firing Clays from Western Georgia. *Interceram* 67, 10–19.
- Biagi, P., Gratuze, B., 2016. New data on source characterization and exploitation of obsidian from the Chikiani area (Georgia). *Eurasistica* 6, 9–35. <https://doi.org/10.14277/6969-093-8/EUR-6-1>.
- Biagi, P., Nisbet, R., Gratuze, B., 2017. Discovery of obsidian mines on Mount Chikiani in the Lesser Caucasus of Georgia. *Antiquity* 91 (357), 1–8. <https://doi.org/10.15184/ajq.2017.39>.
- Chataigner, C., Gratuze, B., 2014a. New data on the exploitation of obsidian in the southern Caucasus (Armenia, Georgia) and Eastern Turkey, Part 1: source characterization. *Archaeometry* 56 (1), 25–47. <https://doi.org/10.1111/arcm.12006>.
- Chataigner, C., Gratuze, B., 2014b. New data on the exploitation of obsidian in the southern Caucasus (Armenia, Georgia) and Eastern Turkey, Part 2: obsidian procurement from the Upper Palaeolithic to the Late Bronze Age. *Archaeometry* 56 (1), 48–69. <https://doi.org/10.1111/arcm.12007>.
- Chilashvili, L. 1970. ქალაქები ფეოდალურ საქართველოში II. [The cities in Feudal Georgia. Vol. II.] Tbilisi. [in Georgian].
- Chilashvili, L., 1999. თბილისის კერამიკული სახელოსნოს დანერგვის ქრონოლოგიის შესახებ. [For the dating of ceramic production center of Tbilisi]. Tbilisi. [in Georgian].
- Coentro, S., Alves, L.C., Relvas, C., Ferreira, T., Mirão, J., Molera, J., Pradell, T., Trindade, R.A.A., Da Silva, R.C., Muralha, V.S.F., 2017. The glaze technology of Hispano-Moresque ceramic tiles: a comparison between Portuguese and Spanish collections. *Archaeometry* 59 (4), 667–684. <https://doi.org/10.1111/arcm.12280>.
- Eramo, G., 2020. Ceramic technology: how to recognize clay processing. *Archaeol. Anthropol. Sci.* 12, 164. <https://doi.org/10.1007/s12520-020-01132-z>.
- Erb-Satullo, N. 2018. Patterns of settlement and metallurgy in Late Bronze–Early Iron Age KvemoKartli, Southern Georgia. In: Anderson, W., Hopper, K., Robinson, A. (eds.), *Landscape Archaeology in Southern Caucasia. Finding Common Ground in Diverse Environments, Proceedings of the workshop held at 10th ICAANE (Vienna, April 2016)*, Austrian Academy of Science Press, pp.37-52.
- Gamkrelidze, I., Gudjbidze, G.E. 2003. Geological map of Georgia. Scale 1:500.000. Georgian State Department of Geology and national Oil Company Saqnavtobi".
- Grigolia, G., Berikashvili, D. 2018. Samshvilde Neolithic Stone Industry. *Archaeology*, vol.2. Tbilisi: The publishing house of the University of Georgia, pp. 87-108.
- Grube, E. 1976. *Islamic Pottery of the Eight-to the Fifteenth century in the Keir Collection*. London.
- Gulmini, M., Giannini, R., Lega, A.M., Manna, G., Mirti, P., 2013. Technology of production of Ghaznavid glazed pottery from bust and Lashkar-i Bazar (Afghanistan). *Archaeometry* 55 (4), 569–590. <https://doi.org/10.1111/j.1475-4754.2012.00703.x>.
- Djaparidze, V. 1956. ქართული კერამიკა (XI-XIII სს.). [Georgian Ceramics. XI-XIIIcc.A.D.]. Tbilisi. [in Georgian].
- Gliozzo, E., 2020a. Ceramics investigation: research questions and sampling criteria. *Archaeol. Anthropol. Sci.* 12, 202. <https://doi.org/10.1007/s12520-020-01128-9>.
- Gliozzo, E., 2020b. Ceramic technology. How to reconstruct the firing process. *Archaeol. Anthropol. Sci.* 12 <https://doi.org/10.1007/s12520-020-01133-y>.

- Hauptmann, A., Klein, S., 2009. Bronze age gold in southern Georgia. *Revue d'archéométrie* 33, 75–82. <https://doi.org/10.4000/archeosciences.2037>.
- Hein, A., Kilikoglou, V., 2020. Ceramic raw materials. How to recognize them and locate the supply basins. *Chemistry. Archaeol. Anthropol. Sci.* 12, 180. <https://doi.org/10.1007/s12520-020-01129-8>.
- Henshaw, C.M. 2010. Early Islamic ceramics and glazes of Akhsiket, Uzbekistan. Doctoral thesis, UCL (University College London).
- Holakooei, P., de LaPérouse, J.F., Carò, F., Röhrs, S., Franke, U., Müller-Wiener, M., Reiche, I., 2019. Non-invasive scientific studies on the provenance and technology of early Islamic ceramics from Afrasiyab and Nishapur. *J. Archaeol. Sci.* 24, 759–772. <https://doi.org/10.1016/j.jasrep.2019.02.029>.
- Ionescu, C., Hoek, V., 2020. Ceramic technology. How to investigate surface finishing. *Archaeol. Anthropol. Sci.* 12, 204. <https://doi.org/10.1007/s12520-020-01144-9>.
- Kavtaradze, G.L. 1999. The importance of metallurgical data for the formation of a Central Transcaucasian chronology. In Hauptmann, A., Pernicka, E., Rehren, Th., Yalçin, Ü. (eds.), *The Beginnings of Metallurgy, Der Anschnitt, Beiheft 9*, pp. 67–101.
- Kibaroglu, M., Satir, M., Kastl, G., 2009. Petrographic and geochemical analysis on the provenance of the Middle Bronze and Late Bronze/Early Iron Age ceramics from Didi Gora and Udabno I, Eastern Georgia. *J. Archaeol. Sci.* 36, 2463–2474. <https://doi.org/10.1016/j.jas.2009.07.005>.
- Klimiashvili, A. 1964. Materials for the history of Kartli and Kakheti administrative units in the 15–18th centuries. Collection: "Several Georgian historic documents of the 15–18th centuries". Tbilisi, pp. 122–123.
- Kopaliani, J. 1996. დმანისის ციხე. [Dmanisi Fortress (historical and archaeological research)]. Tbilisi: Sakartvelo publishers, 1996] Tbilisi. [in Georgian].
- Kuparadze, D., Pataridze, D., Bertolotti, G.P., 2012. Clays of Georgia for ceramic applications. *Interceram* 61, 178–183.
- Kvirkvelia, G., Murvanidze B. 2016. Archaeological Excavations at Grakliani Hill in 2011. Burial mounds of Bronze Period. *Dzhebani* #23. Tbilisi (in Georgian).
- La Russa, M.F., Randazzo, L., Ricca, M., Rovella, N., Barca, D., Ruffolo, S.A., Berikashvili, D., Kvakhadze, L., 2019. The first archaeometric characterization of obsidian artifacts from the archaeological site of Samshilde (South Georgia, Caucasus). *Archaeol. Anthropol. Sci.* 11, 6725–6736. <https://doi.org/10.1007/s12520-019-00936-y>.
- Le Bourdonnec, F.X., Nomade, S., Poupeau, G., Guillou, H., Tushabramishvili, N., Moncel, M.-H., Pleurdeau, D., Agapishvili, T., Voinchet, P., Mgeladze, A., Lordkipanidze, D., 2012. Multiple origins of Bondi Cave and Ortvale Klde (NW Georgia) obsidians and human mobility in Transcaucasia during the Middle and Upper Palaeolithic. *J. Archaeol. Sci.* 39, 1317–1330. <https://doi.org/10.1016/j.jas.2011.12.008>.
- Lomtadize, G. 1988. ქალაქი რუსთავი არქეოლოგიური ძეგლების მიხედვით. [ქალაქი რუსთავი 1946–1965. [Town of Rustavi according to archaeological sites. Archaeological excavations in 1946–1965]. Tbilisi. [in Georgian].
- Martínez Ferreras, V., Fusaro, A., Gurt Esparraguera, J.M., Ariño Gil, E., Pidaev, S.R., Angourakis, A., 2019. The Islamic arrival Termez through the lens of ceramics: A new archaeological and archaeometric study. *Iran*. <https://doi.org/10.1080/05786967.2019.1572430>.
- Mason, R.B., Tite, M.S., 1997. The beginnings of tin opacification of pottery glazes. *Archaeometry* 39 (1), 41–58. <https://doi.org/10.1111/j.1475-4754.1997.tb00789.x>.
- Mason, R.B., Tite, M.S., Paynter, S., Salter, C., 2001. Advances in polychrome ceramics in the Islamic world of the 12th century AD. *Archaeometry* 43 (2), 191–209. <https://doi.org/10.1111/1475-4754.00014>.
- Mindorashvili, D., 2009. არქეოლოგიური გათხრები ძველ თბილისში. [Archaeological Excavations in old Tbilisi]. Tbilisi. [in Georgian].
- Matin, M., 2018. On the origins of tin-opacified ceramic glazes: New evidence from early Islamic Egypt, the Levant, Mesopotamia, Iran, and Central Asia. *J. Archaeol. Sci.* 97, 42–66. <https://doi.org/10.1016/j.jas.2018.06.011>.
- Molera, J., Pradell, T., Salvadó, N., Vendrell-Saz, M., 1999. Evidence of tin oxide recrystallization in opacified lead glazes. *J. Am. Ceram. Soc.* 82 (10), 2871–2875. <https://doi.org/10.1111/j.1151-2916.1999.tb02170.x>.
- Molera, J., Pradell, T., Salvadó, N., Vendrell-Saz, M., 2001. Interactions between clay bodies and lead glazes. *J. Am. Ceram. Soc.* 84 (5), 1120–1128. <https://doi.org/10.1111/j.1151-2916.2001.tb00799.x>.
- Molera, J., Pradell, T., Salvadó, N., Vendrell-Saz, M. 2009. Lead frits in Islamic and Hispano-Moresque glazed productions In: Shortland, A., Freestone, I., Rehren, Th. (Eds.) *From Mine to Microscope. Advances in the study of Ancient materials*. Chapter 1. Oxbow books, pp. 1–11.
- Molera, J., Coll, J., Labrador, A., Pradell, T., 2013. Manganese brown decorations in 10<sup>th</sup> to 18<sup>th</sup> century Spanish tin glazed ceramics. *Appl. Clay Sci.* 82, 86–90.
- Molera, J., Martínez Ferreras, V., Fusaro, A., Gurt Esparraguera, J.M., Gaudenzi, M., Pidaev, S.R., Pradell, T., 2020. Islamic glazed wares from ancient Termez (southern Uzbekistan). Raw materials and techniques. *J. Archaeol. Sci. Rep.* 102169 <https://doi.org/10.1016/j.jasrep.2019.102169>.
- Pradell, T., Molera, J., 2020. Ceramic technology. How to characterise ceramic glazes. *Archaeol. Anthropol. Sci.* 12, 189. <https://doi.org/10.1007/s12520-020-01136-9>.
- Montana, G., 2020. Ceramic raw materials. How to recognize them and locate the supply basins. *Mineralogy, Petrography. Archaeol. Anthropol. Sci.* 12, 175. <https://doi.org/10.1007/s12520-020-01130-1>.
- Pace, M., BiancoPrevot, A., Mirti, P., Venco Ricciardi, R., 2008. The technology of production of Sasanian glazed pottery from Veh Ardašir (central Iraq). *Archaeometry* 50 (4), 591–605. <https://doi.org/10.1111/j.1475-4754.2007.00369.x>.
- Pitskhelauri, K., 1973. The problems for the Eastern Georgian Tribes in the XV–VII centuries BC. Tbilisi [in Georgian].
- Pitskhelauri, K., 2005. *Central Transcaucasian Archaeological culture in the XIV–XIII centuries BC*. Tbilisi. [in Georgian].
- Popkhadze, N., Beridze, T., Moritz, R., Gugushvili, V., Khutsishvili, S., 2009. Facies analysis of the volcano-sedimentary host rocks of the Cretaceous Madneuli massive sulphide deposit, Bolnisi District, Georgia. *Bulletin of the Georgian National Academy of Sciences* 3, 103–108.
- Rezesidze, N. 2011. The settlements of Late Bronze–Early Iron Age from Dmanisi. Georgian National Museum publishing house. Moambe II. (47–B). Tbilisi.
- Sagona, A.G. 2018. *The Archaeology of the Caucasus: From Earliest Settlements to the Iron Age*. Cambridge University Press. Salinas E, Pradell T (2018) The transition from lead transparent to tin-opacified glaze productions in the western Islamic lands: al-Andalus, c. 875–929 CE. *Journal of Archaeological Science* 94:1–11.
- Schillinger, A. 1997. *Die frühesten Zinnbronzen im Schwarzmeerraum*. Magisterarbeit, Universität Tübingen.
- Shaar, R., Tauxe, L., Goguitchaichvili, A., Devidze, M., Licheli, V., 2017. Further evidence of the Levantine Iron Age geomagnetic anomaly from Georgian pottery. *Geophys. Res. Lett.* 44, 2229–2236.
- Shepard, F.P., 1954. Nomenclature based on sand-silt-clay ratios. *J. Sediment. Petrol.* 24, 151–158. <https://doi.org/10.1306/D4269774-2B26-11D7-8648000102C1865D>.
- Sokhadze, G., Floyd, M., Godoladze, T., King, R., Cowgill, E.S., Javakhishvili, Z., Hahubia, G., Reilinger, R., 2018. Active convergence between the Lesser and Greater Caucasus in Georgia: Constraints on the tectonic evolution of the Lesser-Greater Caucasus continental collision. *Earth Planet. Sci. Lett.* 481, 154–161.
- Stöllner, Th., Gambashidze, I. 2014. The Gold Mine of Sakdrisi and early Mining and Metallurgy in Transcaucasia and the Kura-Valley System. In: Narimanishvili, G., Kvachadze, M., Puturidze, M., Shanshashvili, N. (Eds.) *Problems of Early Metal Age Archaeology of Caucasus and Anatolia*. Proceedings of the International Conference (November 19–23, 2014), Tbilisi, pp. 101–124.
- Ting, C., Vionis, A., Rehren, Th., Kassianidou, V., Cook, H., Barker, C., 2019a. The beginning of glazed ware production in late medieval Cyprus. *J. Archaeol. Sci.: Rep.* 27, 101963 <https://doi.org/10.1016/j.jasrep.2019.101963>.
- Ting, C., Lichtenberger, A., Raja, A., 2019b. The technology and production of glazed ceramics from middle Islamic Jerash, Jordan. *Archaeometry* 61 (6), 1296–1312. <https://doi.org/10.1111/arc.12489>.
- Tite, M.S., Freestone, I.C., Mason, R., Molera, J., Vendrell-Saz, M., Wood, N., 1998. Lead glazes in Antiquity - Methods of production and reasons for use. *Archaeometry* 40 (2), 241–260. <https://doi.org/10.1111/j.1475-4754.1998.tb00836.x>.
- Tite, M.S., Pradell, T., Shortland, A., 2008. Discovery, production and use of tin-based opacifiers in glasses, enamels and glazes from the Late Iron Age onwards: a reassessment. *Archaeometry* 50 (1), 67–84. <https://doi.org/10.1111/j.1475-4754.2007.00339.x>.
- Trojsi, G., Positano, M., Palumbi, G., Di Lorenzo, A., 2002. Archaeometrical issues related to Transcaucasian pottery from Georgia. *Periodico di Mineralogia* 71, 239–246.
- Tushishvili, N. 1972. *Madnischalis Cemetery*. Tbilisi. [in Georgian].
- von Suchodoletz, H., Gärtner, A., Hoth, S., Umlauf, J., Sukhishvili, L., Faust, D., 2016. Late Pleistocene river migrations in response to thrust belt advance and sediment-flux steering — The Kura River (southern Caucasus). *Geomorphology* 266, 53–65.
- Yilmaz, A., Adamia, Sh., Chabukiani, A., Chkhotua, T., Erdogan, K., Tuzcu, S., Karabilykoglou, M., 2000. Structural correlation of the southern Transcaucasus (Georgia)-eastern Pontides (Turkey). In: Bozkurt, E., Winchester, J.A., Piper, J.D.A. (eds.), *Tectonics and magmatism in Turkey and the surrounding area*. Geological Society, London, Special Publication 173, pp. 171–182.
- Wilkinson, Ch.K. 1961. *The Glazed Pottery of Nishapur and Samarkand*. The Metropolitan Museum Art Bulletin. New York.
- Wilkinson, Ch.K. 1973. *Nishapur: Pottery of the Early Islamic Period*. New York.